0090-9556/09/3707-1456–1463$20.00
DRUG METABOLISM AND DISPOSITION

DMD 37:1456–1463, 2009

Vol. 37, No. 7
27094/3483322
Printed in U.S.A.

Pharmacokinetic Study of Enclosed Hemoglobin and Outer Lipid Component after the Administration of Hemoglobin Vesicles as an Artificial Oxygen Carrier

Kazuaki Taguchi, Yukino Urata, Makoto Anraku, Toru Maruyama, Hiroshi Watanabe, Hiromi Sakai, Hirohisa Horinouchi, Koichi Kobayashi, Eishun Tsuchida, Toshiya Kai, and Masaki Otagiri

Department of Biopharmaceutics (K.T., Y.U., M.A., T.M., H.W., M.O.), Center for Clinical Pharmaceutical Sciences (T.M., H.W.), and Department of Medical Biopolymer (T.K.), Graduate School of Pharmaceutical Sciences, Kumamoto University, Kumamoto, Japan; Research Institute for Science and Engineering, Waseda University, Tokyo, Japan (H.S., E.T.); Department of Surgery, School of Medicine, Keio University, Tokyo, Japan (K.K., H.H.); and Pharmaceutical Research Center, Nipro Corporation, Shiga, Japan (T.K.)

Received February 11, 2009; accepted April 9, 2009

ABSTRACT:

The hemoglobin vesicle (HbV) is an artificial oxygen carrier that encapsulates a concentrated Hb solution in lipid vesicles (liposomes). The pharmacokinetic properties of HbV were investigated in mice and rats. With use of HbV in which the internal Hb was labeled with ^{125}I (^{125}I-HbV) and cell-free ^{125}I-Hb, it was found that encapsulation of Hb increased the half-life by 30 times, accompanied by decreased distribution in both the liver and kidney. The half-life of HbV was increased, and the uptake clearance for the liver and spleen were decreased with increasing doses of HbV. In an in vitro study, the specific uptake and degradation of HbV in RAW 264.7 cells were found, but this was not the case for parenchymal and endothelial cells. The pharmacokinetics of HbV components (internal Hb and liposomal lipid) were also investigated using ^{125}I-HbV and ^{3}H-HbV (liposomal cholesterol was radiolabeled with tritium-3). The time courses for the plasma concentration curves of ^{125}I-HbV, ^{3}H-HbV, and iron derived from HbV suggest that HbV maintain an intact structure in the blood circulation up to 24 h after injection. ^{125}I-HbV and ^{3}H-HbV were distributed mainly to the liver and spleen. Internal Hb disappeared from both the liver and spleen 5 days after injection, and the liposomal cholesterol disappeared at approximately 14 days. Internal Hb was excreted into the urine and cholesterol into feces via biliary excretion. These results suggest that the HbV has a reasonable blood retention and metabolic and excretion performance and could be used as an oxygen carrier.

Blood transfusions are absolutely essential for resuscitation from massive bleeding after a surgical procedure. However, there is the potential of mismatching, and they can introduce certain infectious diseases such as hepatitis, human immunodeficiency virus, or West Nile virus, which are threats despite the development of the nucleic acid amplification test. In addition, donated red blood cells (RBCs) for blood transfusions can only be stored for a period of 3 weeks in Japan. To overcome these problems, blood substitutes would be highly desirable and have been under development worldwide (Keipert, 1995; Winslow, 2005).

The hemoglobin vesicle (HbV) is an artificial cellular hemoglobin-based oxygen carrier with polyethylene glycol (PEG), in which phospholipid vesicles encapsulating highly concentrated human Hb serve as oxygen carriers with oxygen transport characteristics that are comparable to those of RBCs. In fact, the pharmacological effects of HbV, injected into rats with hemorrhagic shock, have been reported to be equivalent to those of RBCs (Sakai et al., 2004b, 2009). In addition, HbV have been shown to possess a number of positive characteristics such as the absence of viral contamination (Sakai et al., 1993; Abe et al., 2006), a long-term storage period of more than 2 years at room temperature (Goda et al., 1998; Sakai et al., 2000b; Abe et al., 2007), and low toxicity [blood compatibility, and suppressed nephrotoxicity induced by the dimeric form of Hb and hypertension induced by the direct interaction of Hb with nitric oxide (NO) and

This work was supported in part by the Ministry of Health, Labour and Welfare, Japan [Health Science Research Grants (Health Science Research Including Drug Innovation)].

K.T. and Y.U. contributed equally to this work.

Article, publication date, and citation information can be found at http://dmd.aspetjournals.org.

doi:10.1124/dmd.109.027094.

ABBREVIATIONS: RBC, red blood cell; HbV, hemoglobin vesicle(s); PEG, polyethylene glycol; NO, nitric oxide; ^{125}I-HbV, ^{125}I-labeled hemoglobin vesicle; ^{3}H-HbV, ^{3}H-labeled hemoglobin vesicle; DPPC, 1,2-dipalmitoyl-*sn*-glycero-3-phosphatidylcholine; rHSA, recombinant human serum albumin; BSA, bovine serum albumin; TCA, trichloroacetic acid; PBS, phosphate-buffered saline; WE, Williams' E medium; FCS, fetal calf serum; AUC, area under the concentration-time curve; MPS, mononuclear phagocyte system; ID, injected dose; Hp, haptoglobin; CL_{uptake}, uptake clearance.

CO] (Sakai et al., 2000a). Moreover, HbV suspended in a solution of human serum albumin can be used to regulate rheological properties (e.g., viscosity and colloid osmotic pressure) (Sakai et al., 2000c, 2004b). On the basis of these facts, the use of HbV is predicted to be superior to that of a conventional blood transfusion.

Preclinical pharmacokinetic studies of HbV are essential to evaluate the safety and efficacy of HbV. To sustain the pharmacological effect of HbV as artificial oxygen carriers, prolonged oxygen delivery is a required property. In fact, the plasma retention time of free Hb, when isolated from RBCs, is surprisingly short (half-life of ~0.5–1.5 h). In clinical situations, the total infused dose of RBCs given to patients can be considerable (e.g., for hemorrhagic shock or transfusion during an operation). Because the lipid content of HbV is more than 100 times higher than that of other liposomal preparations such as AmBisome or Doxil, massive amounts of Hb and lipid components can be infused when HbV are substituted for RBCs.

Free Hb molecules can trigger numerous side effects, such as renal toxicity, hypertension, and tissue damage induced by the Fenton reaction, which is mediated by heme (iron) (Balla et al., 2005). On the other hand, high levels of lipid components in the bloodstream, especially cholesterol, are risk factors for kidney disease, arterial sclerosis, and hyperlipidemia (Gröne and Gröne, 2008). Despite the large body of pharmacological evidence for the HbV as an artificial oxygen carrier, little is known concerning its pharmacokinetic properties, especially the fate of each component after injection. As of this writing, metabolism studies of HbV components have only been done by histopathological examination and blood serum biochemistry (Sakai et al., 2001, 2009). However, it is difficult to distinguish exogenous lipid components, derived from HbV, from endogenous substances. Biodistribution of HbV has been examined by ^{99m}Tc-labeled HbV (Sou et al., 2005); however, no pharmacokinetic studies of Hb and lipids from administration to excretion were performed.

In the present study, we report on an evaluation of the pharmacokinetic properties of the HbV and its components, from the standpoint of stability in the blood circulation and the metabolism and excretion of each component, in support of its use as an oxygen carrier. For this purpose, we used two different radiolabeled HbV, ^{125}I-HbV in which the enclosed Hb was radiolabeled and ^{3}H-HbV in which the lipid component (cholesterol) was radiolabeled.

Materials and Methods

Materials. An Hb solution was purified from outdated donated blood that was provided by the Japanese Red Cross Society (Tokyo, Japan). Pyridoxal 5′-phosphate was purchased from Sigma-Aldrich (St. Louis, MO). 1,2-Dipalmitoyl-*sn*-glycero-3-phosphatidylcholine (DPPC), cholesterol, and 1,5-bis-*O*-hexadecyl-*N*-succinyl-L-glutamate were purchased from Nippon Fine Chemical Co. Ltd. (Osaka, Japan). 1,2-Distearoyl-*sn*-glycero-3-phosphatidylethanolamine-*N*-PEG was purchased from NOF Corporation (Tokyo, Japan). Recombinant human serum albumin (rHSA) was given by NIPRO (Osaka, Japan). Williams' E medium (WE medium) and RPMI 1640 medium were purchased from Sigma-Aldrich. Dulbecco's modified Eagle's medium and penicillin-streptomycin were purchased from Invitrogen (Carlsbad, CA).

Preparation of HbV. HbV were prepared under sterile conditions as reported previously (Sakai et al., 1997). The resulting encapsulated Hb (38 g/dl) contained 14.7 mM pyridoxal 5′-phosphate as an allosteric effector to regulate P_{50} to 25 to 28 Torr. The lipid bilayer comprised a mixture of DPPC, cholesterol, and 1,5-bis-*O*-hexadecyl-*N*-succinyl-L-glutamate at a molar ratio of 5:5:1 and 1,2-distearoyl-*sn*-glycero-3-phosphatidyl-ethanolamine-*N*-PEG (0.3 mol%). The averaged particle diameter was 250 to 280 nm. The HbV were suspended in a physiological salt solution at [Hb] (10 g/dl) and [lipids] (6–7 g/dl), filter-sterilized (450 nm pore size, Dismic; Toyo-Roshi, Tokyo, Japan), and purged with N_2 before storage.

In Vivo Experiment. *Animals.* All animal experiments were undertaken in accordance with the guideline principles and procedures of Kumamoto University for the care and use of laboratory animals. Experiments were performed with male ddY mice (28–30 g b.wt.; Japan SLC, Inc., Shizuoka, Japan) and male Sprague-Dawley rats (180–210 g b.wt.; Kyudou Co., Kumamoto, Japan). All animals were maintained under conventional housing conditions, with food and water ad libitum in a temperature-controlled room with a 12-h dark/light cycle. Before the pharmacokinetic studies using ^{125}I-Hb or ^{125}I-HbV, all of the animals were given water containing 5 mM sodium iodide (NaI) to avoid specific accumulation of the isotope in the glandula thyreoidea until the end of the experiment.

Preparation of radiolabeled Hb and HbV. ^{125}I-Hb or ^{125}I-HbV were prepared by incubating 200 μl of Hb or HbV (100 mM Hb) with 125-I as Na^{125}I (10 μl) (GE Healthcare, Little Chalfont, Buckinghamshire, UK) in an Iodo-Gen (1,3,4,6-tetrachoro-3α,6α-diphenylglycoluril) tube for 30 min at room temperature. ^{125}I-Hb and ^{125}I-HbV were then isolated from free ^{125}I by passage through a PD-10 column (Pfizer, Inc., Uppsala, Sweden). More than 97% of the total iodine was bound to internal Hb in HbV. ^{3}H-HbV were prepared by mixing HbV (1 ml) with [1,2-^{3}H]cholesterol solution (40 μl) (PerkinElmer Life and Analytical Sciences, Yokohama, Japan) and incubated for 12 h at room temperature. ^{3}H-HbV were filtered through a sterilized filter to remove aggregates (pore size, 450 nm). The incubation of ^{3}H-HbV in serum (24 h, 37°C) revealed that ^{3}H failed to completely dissociate from the HbV. Before use in pharmacokinetic experiments, all of the samples were mixed with unlabeled protein (Hb or HbV) to adjust the target Hb concentration. In addition, rHSA was added to correspond to the colloid osmotic pressure (Sakai et al., 1997).

Administration and collection of blood and organs in mice. ddY mice received a single injection of ^{125}I-Hb (1 mg of Hb/kg), ^{125}I-HbV (1, 10, 200, and 1400 mg of Hb/kg), or ^{3}H-HbV (1400 mg of Hb/kg) containing 5% rHSA in the tail vein under ether anesthesia. At each time after the injection of labeled protein, blood was collected from the inferior vena cava, and plasma was obtained by centrifugation (3000*g*, 5 min). After collection of blood, the animal was sacrificed for excision of organs. Urine and feces were collected at fixed intervals in a metabolic cage.

Administration and collection of blood and organs in rats. All of the Sprague-Dawley rats were anesthetized with pentobarbital and received a single injection of ^{125}I-HbV (10, 200, and 1400 mg of Hb/kg) or ^{3}H-HbV (1400 mg of Hb/kg) containing 5% rHSA. The blood was collected from the tail vein, and plasma was obtained by centrifugation (3000*g*, 5 min). At each time after an injection of ^{125}I-HbV or ^{3}H-HbV, the three animals were sacrificed for collection of organs, which were rinsed with saline. Urine and feces were collected at fixed intervals in a metabolic cage.

Measurement of ^{125}I radioactivity. To remove degraded protein and free ^{125}I, 1% bovine serum albumin (BSA) and 40% trichloroacetic acid (TCA) were added to the plasma, and pellets were obtained by centrifugation (1000*g*, 10 min). The organs, urine, and feces were weighed on an electronic balance. ^{125}I radioactivity was counted using a liquid scintillation counter (ARC-5000; Aloka, Tokyo, Japan).

Measurement of ^{3}H radioactivity. The plasma samples were ultracentrifuged to collect intact HbV (50,000*g*, 30 min) (Sakai et al., 2001). Collected HbV were solubilized in a mixture of Soluene 350 (PerkinElmer Life and Analytical Sciences) and isopropyl alcohol (at a ratio of 1:1) for 24 h at 50°C and decolorized by treatment with H_2O_2. The organ samples were rinsed with saline, minced, and solubilized in Soluene 350 for 24 h at 50°C. Urine and feces were also weighed and solubilized in Soluene 350. Radioactivity was determined using a liquid scintillation counter (LSC-5121; Aloka) with Hionic-Fluor (PerkinElmer Life and Analytical Sciences).

Measurement of iron concentration. The iron concentration was calculated from atomic emission spectrometric analysis (Ubest-35; Jasco, Tokyo, Japan) using an absorbance of 415 nm. The specific iron concentration derived from HbV was calculated by subtraction of the plasma iron concentration without HbV injection from that with HbV injection. At the same time, we confirmed that the plasma iron level hardly changed without HbV in mice during the experimental periods.

In Vitro Experiment. *Separation of hepatic cells.* Separation of hepatic cells from ddY mice was performed using a method similar to that described in a previous report (Nakajou et al., 2005). The portal vein was cannulated with a polyethylene catheter, and the liver was perfused with Gey's balanced salt solution buffer, pH 7.5, without Ca^{2+} for 10 min at flow rate of 5 ml/min and

then with Gey's balanced salt solution buffer, pH 7.5, containing 125 units/ml collagenase and Ca^{2+} for 3 min at 37°C. The liver was suspended in ice-cold 1% BSA. The cell suspension was centrifuged at 20*g* for 2 min, and the precipitate and supernatant were collected. Parenchymal and endothelial cells were isolated from the precipitate and supernatant as follows.

Isolation and culture of hepatic parenchymal cells. The precipitate was resuspended in 1% BSA and again centrifuged at 20*g* for 2 min. The cells in the pellet were resuspended in 10 ml of phosphate-buffered saline (PBS) and layered on top of a two-step Percoll gradient. The gradient consisted of 25% (v/v) Percoll (top) and 50% (v/v) Percoll (bottom). The gradient was centrifuged at 3000*g* for 30 min, and the intermediate zone was collected. The enriched hepatic parenchymal cells were suspended in WE medium (FCS+) supplemented with 0.1 mg/ml streptomycin and 100 IU/ml penicillin. Aliquots of the cell suspension were seeded into each well (5×10^5 per well) of collagenase-coated 24-multiwell plates. The multiwell plates were incubated for 60 min at 37°C in a CO_2 incubator. Each well was washed three times with 1 ml of PBS to remove nonadherent cells, and then further incubated for 12 h with 1 ml of WE medium (FCS+), which was replaced by 1 ml of fresh WE medium (FCS−), followed by a 4-h incubation before the experiment.

Isolation and Culture of Hepatic Endothelial Cells. The supernatant was suspended in 10 ml of RPMI 1640 medium (FCS−) and cultured on a plastic plate for 20 min (37°C) to remove Kupffer cells. The supernatant in the plastic plate was then seeded into each well (2×10^6 per well) of fibronectin-coated 24-multiwell plates. The multiwell plates were incubated for 60 min at 37°C in a CO_2 incubator. Each well was washed twice with 1 ml of PBS to remove nonadherent cells and parenchymal cells and then further incubated for 2 h with 1 ml of RPMI 1640 medium (FCS+), which was replaced by 1 ml of fresh RPMI 1640 medium (FCS−), followed by a 4-h incubation before the experiment.

Culture of RAW 264.7 cells. RAW 264.7 cells suspended in Dulbecco's modified Eagle's medium (FCS+) were seeded into each well (5×10^5 per well) of 24-multiwell plates. The multiwell plates were incubated for 24 h at 37°C in a CO_2 incubator. Each well was washed twice with 1 ml of PBS, which was replaced by 1 ml of fresh Dulbecco's modified Eagle's medium (FCS−), followed by a 4-h incubation before the experiment.

Cell assays. The parenchymal, endothelial, and RAW 264.7 cells in each well were incubated with various concentrations of ^{125}I-HbV for examination, with or without an excess of corresponding unlabeled HbV. After a 6-h incubation, 0.575 ml of culture medium was removed from each well and mixed with 0.15 ml of 40% TCA and 0.15 ml of 0.7 M $AgNO_3$ in a vortex mixer, followed by centrifugation (1000*g*, 10 min). The resulting supernatant (0.25 ml) was used to determine TCA-soluble radioactivity, which was taken as an index of the extent of cellular degradation. The remaining cells in each well were washed five times with 1 ml of PBS. The cells were lysed at 37°C for 30 min with 1 ml of 0.1 M NaOH. One portion was used to determine the radioactivity as the cell-associated ligand; the other was used to determine the cellular protein content.

Data analysis. Pharmacokinetic analyses after HbV or Hb administration was performed based on a two-compartment model. Pharmacokinetic parameters were calculated by fitting using MULTI, a normal least-squares program (Yamaoka et al., 1981). The uptake clearance (CL_{uptake}) was calculated, as described in a previous report using integration plot analysis at designated times (from 1 to 30 min) during which the efflux and/or elimination of radioactivity from tissues were negligible (Murata et al., 1998). Data are shown as mean ± S.D. for the indicated number of animals. The overall differences between groups were determined by one-way analysis of variance. A value of $p < 0.05$ was considered to indicate statistical significance.

Results

Comparison of Pharmacokinetic Properties between Hb and HbV. The fates of the ^{125}I-Hb and ^{125}I-HbV administered to mice were evaluated as residual TCA-precipitable radioactivity in the plasma. Figure 1A shows the time courses for the plasma concentrations of ^{125}I-Hb and ^{125}I-HbV in mice at a dose of 1 mg of Hb/kg. The blood circulation of HbV was increased notably. According to the pharmacokinetic parameters based on a two-compartment model analysis, the clearance of ^{125}I-HbV was significantly decreased (3.4 ± 0.1 ml/h) compared with that of ^{125}I-Hb (12.7 ± 2.1 ml/h, $p < 0.001$). The half-life ($t_{1/2}$) and the area under the concentration-time curve (AUC) of ^{125}I-HbV were increased ($t_{1/2}$, 3.1 ± 1.0 and 0.1 ± 0.1 h, $p < 0.01$ and AUC, 29.4 ± 9.2 and 7.9 ± 3.9 h · % dose/ml, $p < 0.001$, for ^{125}I-HbV and ^{125}I-Hb, respectively) with decreasing clearance, whereas the distribution volume (V_1) remained unchanged (2.3 ± 0.1 and 2.6 ± 0.3 ml for ^{125}I-HbV and ^{125}I-Hb, respectively). Figure 1B shows the tissue distribution in each organ at 3 min after an injection of ^{125}I-Hb or ^{125}I-HbV. As expected, ^{125}I-Hb was distributed mainly in the kidney and liver. In contrast, the distribution of ^{125}I-HbV was significantly decreased, whereas its distribution in the spleen and lung was increased significantly.

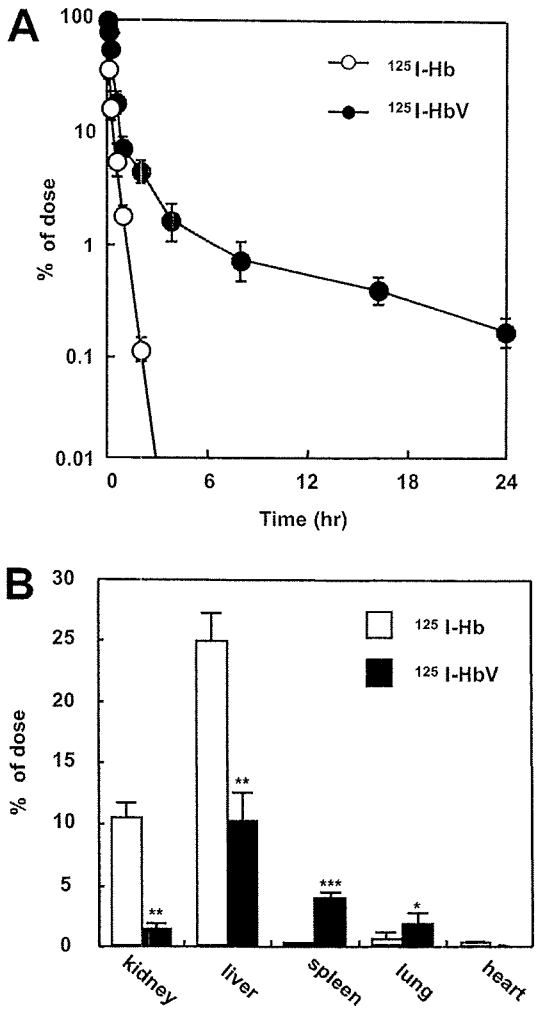

FIG. 1. A, time course for the plasma level of ^{125}I-Hb (○) and ^{125}I-HbV (●) after administration to mice. ddY mice received a single injection of ^{125}I-Hb or ^{125}I-HbV from the tail vein at a dose of 1 mg/kg. Blood was collected from the inferior vena cava under ether anesthesia, and a plasma sample was obtained. Each point represents the mean ± S.D. (n = 3–6). B, tissue distributions of ^{125}I-Hb (□) and ^{125}I-HbV (■) at 3 min after administration to mice. ddY mice received a single injection of ^{125}I-Hb or ^{125}I-HbV from the tail vein at a dose of 1 mg/kg. At 3 min after injection, each organ was collected. Each bar represents the mean ± S.D. (n = 3–6). *, $p < 0.05$, **, $p < 0.01$, and ***, $p < 0.001$ versus ^{125}I-Hb.

Dose Dependence of HbV Pharmacokinetics. Table 1 shows the pharmacokinetic parameters for ^{125}I-HbV administered to mice at doses of 1, 10, 200, and 1400 mg of Hb/kg. As the dose was increased, $t_{1/2\beta}$ was increased and clearance was decreased. The AUC was increased in proportion to $t_{1/2\beta}$. Table 2 shows the dose-dependent CL_{uptake} in each organ. CL_{uptake} in liver and spleen was much

TABLE 1

Dose-dependent pharmacokinetic parameters of HbV after administration of ^{125}I-HbV in mice

All mice received a single injection of ^{125}I-HbV (1, 10, 200, and 1400 mg of Hb/kg) containing 5% rHSA. At each time (0.05, 0.5, 1, 2, 4, 6, 8, 12, and 24 h) after the ^{125}I-HbV injection, blood samples were collected from the inferior vena cava, and a plasma sample was obtained. Each parameter was calculated by MULTI using a two-compartment model. Values are mean ± S .D. (n = 3–6).

	Dose			
	1 mg of Hb/kg	10 mg of Hb/kg	200 mg of Hb/kg	1400 mg of Hb/kg
$t_{1/2\beta}$ (h)	3.1 ± 3.1	3.6 ± 1.3	7.2 ± 3.1	18.8 ± 1.3
AUC (hr · % dose/ml)	29.4 ± 7.2	32.9 ± 3.8	134 ± 42	829 ± 38
Clearance (ml/h)	3.40 ± 0.1	3.04 ± 0.1	0.74 ± 0.1	0.12 ± 0.1
V_1 (ml)	2.35 ± 0.2	2.43 ± 0.3	2.24 ± 0.2	1.75 ± 0.6

TABLE 2

Dose-dependent uptake clearance of HbV in liver, spleen, kidney, lung, and heart after ^{125}I-HbV administration in mice

All mice received a single injection of ^{125}I-HbV (1, 10, 200, and 1400 mg of Hb/kg) containing 5% rHSA. The uptake clearance for each organ was calculated by integration plot analysis at designated times from 1 to 30 min after injection. Values are mean ± S.D. (n = 3–6).

Dose	CL_{uptake}				
	Liver	Spleen	Kidney	Lung	Heart
			μl/h		
1 mg of Hb/kg	2608 ± 654	1018 ± 188	19 ± 9.4	3.5 ± 0.9	0.14 ± 0.06
10 mg of Hb/kg	1473 ± 440	786 ± 94	18 ± 8.1	2.5 ± 0.2	0.38 ± 0.09
200 mg of Hb/kg	452 ± 114	102 ± 36	25 ± 9.2	1.3 ± 0.2	0.06 ± 0.02
1400 mg of Hb/kg	256 ± 37	51 ± 6.1	27 ± 9.4	0.6 ± 0.2	0.14 ± 0.06

higher than that in the other organs. As the dose was increased, CL_{uptake} in liver and spleen was decreased. These results suggested that the distribution of HbV to the liver and spleen, which contained the majority of HbV, was saturated at higher doses.

Cell Assay. It is well known that liposomes are scavenged and degraded by the mononuclear phagocyte system (MPS), such as Kupffer cells or macrophages (Kiwada et al., 1998). Because HbV were distributed mainly in the liver and spleen, where the MPS is localized, we examined the issue of whether HbV are scavenged and degraded by MPS using RAW 264.7 cells, which have been used as an alternative to Kupffer cells. In these experiments, primary parenchymal and endothelial cells from mouse livers were used as a control. As shown in Fig. 2, the specific uptake and degradation of ^{125}I-HbV were observed only in the RAW 264.7 cells and not in primary parenchymal and endothelial cells. This in vitro study supports the fact that HbV are captured by Kupffer cells in the liver and by macrophages in the red pulp zone of the spleen, as reported previously in an in vivo study (Sakai et al., 2001).

Pharmacokinetics of HbV Components in Mice. To investigate the pharmacokinetics of each HbV component, Hb, enclosed in HbV, was radiolabeled with ^{125}I (^{125}I-HbV) or cholesterol, in the lipid component vesicles of HbV, was radiolabeled with ^{3}H (^{3}H-HbV). As

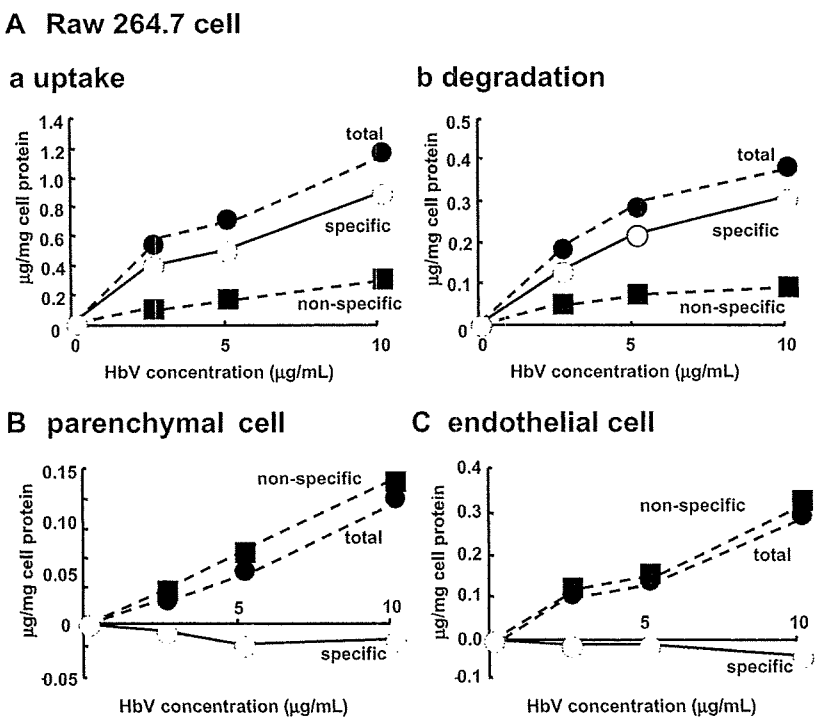

FIG. 2. A, dose-dependent endocytic uptake (a) and degradation (b) of ^{125}I-HbV by RAW 264.7 cells. B and C, endocytic uptake of ^{125}I-HbV by parenchymal cells and endothelial cells, respectively. RAW 264.7, primary parenchymal, and endothelial cells were incubated at 37°C for 6 h with the indicated concentration of ^{125}I-HbV in the presence (■) or absence (●) of 50-fold unlabeled HbV. Specific uptake or degradation (○) was calculated by subtracting the nonspecific values from the total values. Results are the mean ± S.D. of three separate experiments.

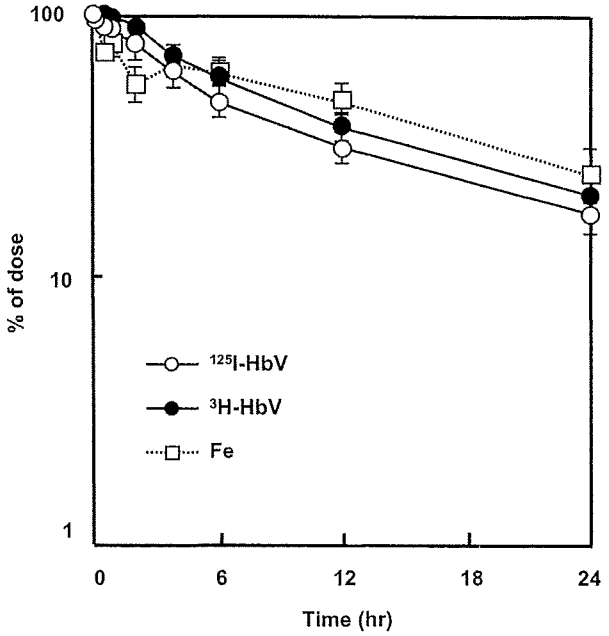

FIG. 3. Time course for the plasma level of ^{125}I-HbV (○), ^{3}H-HbV (●), and iron (□) derived from HbV after administration to mice. ddY mice received a single injection of ^{125}I-HbV or ^{3}H-HbV from the tail vein at a dose of 1400 mg of Hb/kg. Blood was collected from the inferior vena cava under ether anesthesia, and a plasma sample was obtained. The iron concentration was calculated from atomic emission spectrometric analysis using an absorbance of 415 nm. Each point represents the mean ± S.D. (n = 3–6).

shown in Fig. 3 and Table 3, similar plasma concentration curves and pharmacokinetic parameters of ^{125}I-HbV were observed for ^{3}H-HbV. Furthermore, after administration of nonlabeled HbV to mice, the time course for the plasma iron concentration curve derived from HbV was consistent with the plasma concentration curves for both labeled HbV (Fig. 3). These data indicate that HbV is likely to maintain an intact structure in the blood circulation for periods of up to 24 h after injection. We also examined the issue of whether the injected HbV had any influence on the production of reactive oxidative species because, if free iron were released from vesicles, it would enhance the production of ROS by the Fenton reaction, as has been previously demonstrated (Anraku et al., 2004, 2008). To quantitatively evaluate the extent of oxidative stress in the blood circulation, we monitored the ratio of the mercapt-form (nonoxidized form) to the nonmercapt-form (oxidized form) of serum albumin, which serves as a marker of oxidative stress in the circulatory system (Kadowaki et al., 2007; Shimoishi et al., 2007). No significant differences in these ratios were found between HbV and the saline administration groups for periods of up to 7 days after administration (data not shown).

Moreover, the tissue distribution of ^{125}I-HbV was evaluated using the tissue-to-plasma partition coefficient (K_p). Figure 4 shows the K_p values in organs (kidney, liver, spleen, lung, and heart) 8 h after the administration of ^{125}I-HbV or ^{3}H-HbV to mice. Among these organs, the K_p values for both the liver and spleen reached >1 for both radiolabeled HbV. Therefore, we examined the time course for the tissue distribution in the liver (Fig. 5A) and spleen (Fig. 5B) after the administration of both labeled HbV. At an early time period (Fig. 5, A and B, insets), the time course distributions for ^{125}I-HbV and ^{3}H-HbV were consistent with each other, and the CL_{uptake} values in liver and spleen were also similar (liver, 256 ± 37 and 301 ± 41 μl/h and spleen, 51 ± 6 and 43 ± 12 μl/h for ^{125}I-HbV and ^{3}H-HbV, respectively). However, the radioactive ^{125}I was more rapidly eliminated from each organ, and the activity essentially disappeared within 7 days. On the other hand, the elimination of radioactive ^{3}H was delayed compared with that of ^{125}I and nearly disappeared after 14 days in both liver and spleen. These data indicate that HbV was distributed mainly to liver and spleen in the form of intact HbV and that it was degraded by MPS, followed by different routes of excretion for the internal Hb and the lipid component.

To identify the excretion pathway of HbV, the levels of radioactivity ^{125}I and ^{3}H in urine and feces were measured (Fig. 6). The radioactive ^{125}I was excreted mainly in the urine (84.2 ± 4.1% of ID at 7 days after injection), but was low in feces (5.1 ± 2.3% of ID at 7 days after injection). In addition, neither Hb nor protein urea nor hemoglobinuria was detected in the urine (data not shown). On the other hand, the majority of the radioactive ^{3}H was excreted in the feces (71.1 ± 3.6% of ID at 7 days after injection), and a small portion was excreted into the urine (19.8 ± 3.4% of ID at 7 days after injection). At 7 days after injection, a high level of radioactivity from ^{3}H was detected in plasma lipoprotein and bile, but ^{125}I was not (data not shown).

Pharmacokinetics of the HbV Component in Rats. Because altered pharmacokinetics of liposomes have been reported for different animal species, we carried out a pharmacokinetic analysis in rats as well. The rats showed dose dependence for HbV pharmacokinetics similar to that observed for mice, except that the half-life of HbV was doubled ($t_{1/2}$ of 8.8 ± 0.7, 11.5 ± 0.3, and 30.6 ± 4.0 h at doses of 10, 200, and 1400 mg of Hb/kg, respectively).

Table 3 shows data for the pharmacokinetic analysis of ^{125}I- and ^{3}H-HbV in rats. Although the pharmacokinetic behaviors of both radiolabeled HbV were similar to those for mice, the maximum hepatic distributions of labeled HbV in rats were decreased by nearly half of those in mice (13.5 ± 0.5 and 17.7 ± 3.0% of ID for ^{125}I-HbV and ^{3}H-HbV, respectively). Moreover, the radioactive ^{125}I was excreted mainly in the urine (77.9 ± 6.1 and 4.8 ± 1.6% of ID at 7 days after injection for urine and feces, respectively). On the other hand, the majority of the radioactivity of ^{3}H was excreted into feces (10.9 ± 4.4 and 66.3 ± 14.8% of ID at 7 days after injection for urine and feces, respectively).

Discussion

The HbV has been developed as an artificial oxygen carrier and has considerable promise for use in clinical settings because of its superb functionality, such as its ability to regulate rheological properties and cardiocirculatory dynamics and its oxygen carrier ability (Izumi et al., 1996; Sakai et al., 2008). In previous studies, cell-free Hb and perfluorocarbon, which had also been developed for use as artificial oxygen carriers, were excluded as possible candidates, because their systemic half-lives were too short (~0.5–1.5 h) or long (1 year or longer), respectively, for them to effectively function as an optimal oxygen carrier (Savitsky et al., 1978; Nosé, 2004). Therefore, it is necessary to characterize the pharmacokinetic properties of the HbV and its components to demonstrate the efficacy and safety of this preparation because a short half-life leads to a diminished pharmacological effect, whereas a long half-life increases the bioaccumulative potential.

In this study, the half-life of HbV was found to be 30 times higher than that of stroma-free Hb at a dose rate of 1 mg Hb/kg due to decreased distribution to the liver and kidney (Fig. 1). This finding could reflect physicochemical differences, such as diameter, the absence or presence of a membrane structure, and PEG modification between HbV and Hb. In physiological conditions, Hb that is released from ruptured RBCs becomes rapidly bound to haptoglobin (Hp), which promotes CD163 recognition in the liver (Kristiansen et al., 2001). When the Hb concentration exceeds the Hp-binding capacity,

TABLE 3

Pharmacokinetic parameters of HbV after administration of ^{125}I- and ^{3}H-HbV in mice and rats

All mice and rats received a single injection of ^{125}I-HbV or ^{3}H-HbV at a dose of 1400 mg of Hb/kg containing 5% rHSA. At each time after the injection of ^{125}I-HbV or ^{3}H-HbV, a blood sample was collected from the inferior vena cava (mice) or from the tail vein (rats), and plasma was obtained. Each parameter was calculated by MULTI using a two-compartment model. Values are mean ± S.D. (n = 3–6).

	Mice		Rats	
	^{125}I-HbV	^{3}H-HbV	^{125}I-HbV	^{3}H-HbV
$t_{1/2\beta}$ (h)	18.8 ± 1.3	19.9 ± 0.9	30.6 ± 4.0	30.9 ± 4.7
AUC (hr · % dose/ml)	829 ± 28	899 ± 44	210 ± 23	247 ± 22
Clearance (ml/h)	0.12 ± 0.04	0.11 ± 0.03	0.46 ± 0.04	0.41 ± 0.02
V_1 (ml)	1.75 ± 0.6	1.71 ± 0.1	10.9 ± 0.2	10.2 ± 2.0

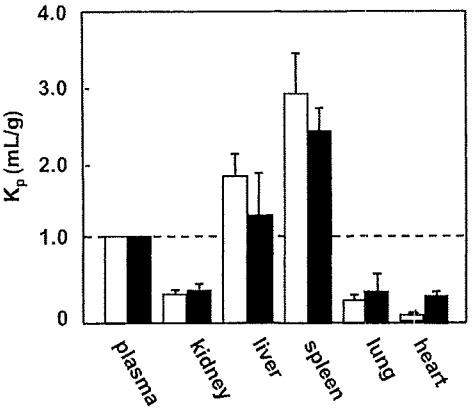

FIG. 4. The tissue-to-plasma partition coefficient (K_p) of ^{125}I-HbV (□) and ^{3}H-HbV (■) 8 h after administration to mice. Each bar represents the mean ± S.D. (n = 6).

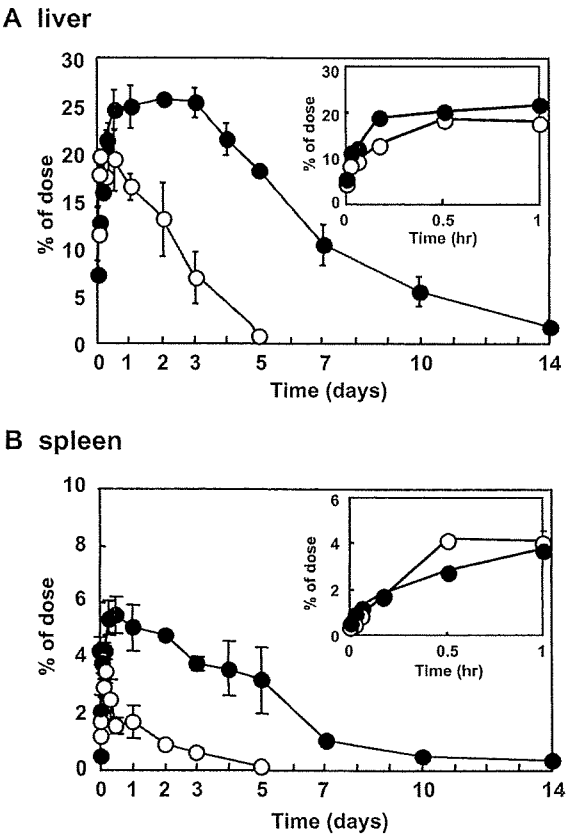

FIG. 5. Time course for radioactivity in liver (A) and spleen (B) after the administration of ^{125}I-HbV (○) or ^{3}H-HbV (●) at a dose of 1400 mg of Hb/kg to mice. ddY mice received a single injection of ^{125}I-HbV or ^{3}H-HbV from the tail vein at a dose of 1400 mg of Hb/kg. Each point represents the mean ± S.D. (n = 3–6).

unbound Hb is filtered through the kidney (Savitsky et al., 1978). Thus, the reduction in HbV distribution in the liver and kidney could be due to the encapsulation of Hb by the liposome because it may not only suppress the binding of internal Hb to Hp but also inhibit renal glomerular filtration.

For HbV, approximately 10% of the dose was distributed to the liver. Because HbV possess a liposome structure, they would be expected to be captured by MPS in the liver and spleen (Kiwada et al., 1998). In fact, as the dose is increased, CL_{uptake} in the liver and spleen was decreased (Table 2), and the half-life was increased (Table 1). In addition, specific uptake and degradation were observed only in macrophage cells but not in parenchymal and endothelial cells (Fig. 2). These results strongly suggest that HbV are scavenged by the MPS, such as Kupffer cells or the red pulp zone, and that this ability became saturated at high doses of HbV. These results are in reasonably good agreement with previous in vivo findings that HbV are taken up by Kupffer cells, the red pulp zone, and mesangial cells (Sakai et al., 2001, 2004a). However, because of increased distribution of HbV into spleen and lung compared with that of free Hb, further study will be needed to demonstrate the effect of HbV administration on the immune and respiratory systems.

In clinical situations such as hemorrhagic shock or an intensive surgical procedure, a massive dose of HbV would be administered to patients. Therefore, it is important to confirm the safety of HbV components from the viewpoint of pharmacokinetics, because Hb molecules can trigger a number of side effects such as renal toxicity and hypertension derived by scavenging endothelium-derived NO (synthesized by NO synthase-3) (Yu et al., 2008) and tissue damage induced by the Fenton reaction mediated by heme (iron) (Balla et al., 2005). In addition, the long-term circulation of high amounts of lipids, especially cholesterol, contributes to cardiovascular and kidney disease (Gröne and Gröne, 2008). In this study, we were able to confirm the safety of HbV components, including Hb, iron, and lipids, based on pharmacokinetic analyses, as evidenced by the following procedures.

First, the findings herein clearly showed that for up to 24 h after injection, the plasma concentration curves of ^{125}I-HbV, ^{3}H-HbV, and iron derived from HbV exhibited similar behaviors (Fig. 3). In addition, CL_{uptake} in liver and spleen was also similar for ^{125}I-HbV and ^{3}H-HbV (see *Results*). These results indicate that the HbV circulates in the bloodstream as stable, intact vesicles until degraded by the MPS.

Second, nearly 80% of the radioactive ^{125}I is excreted into the urine by 7 days after its injection. This radioactivity is probably due to the degradation of Hb enclosed in liposomes because ^{125}I binds covalently to tyrosine residues of protein (Burger et al., 1983). In fact,

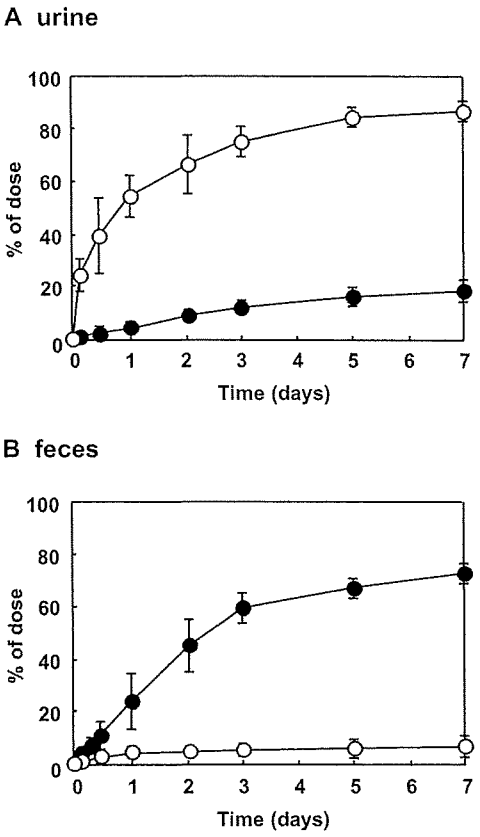

FIG. 6. Time course for radioactivity in urine (A) and feces (B) after the administration of ^{125}I-HbV (○) and ^{3}H-HbV (●) to mice. ddY mice received a single injection of ^{125}I-HbV or ^{3}H-HbV from the tail vein at a dose of 1400 mg of Hb/kg. Urine and feces were collected at fixed intervals in a metabolic cage. Each point represents the mean ± S.D. (n = 3–6).

neither Hb nor protein urea nor hemoglobinuria was detected in the urine. Moreover, a previous study showed that multiple-dose or a single high-dose treatment of HbV failed to induce any detectable pathological injury in the kidney or any change in arteriolar or venular diameters, which are induced by the dimeric form of Hb or any direct interaction of Hb with NO (Sakai et al., 2001, 2004a; Cabrales et al., 2005). These results indicate that ^{125}I-HbV are degraded by the MPS and that the ^{125}I is excreted in the urine in the form of a degradation product of ^{125}I-Hb derived from HbV.

Third, an excess of heme (iron) could cause hemosiderosis and oxidative stress via the Fenton reaction (Buehler and Alayash, 2004). Therefore, the disposition of heme (iron) derived from HbV needs to be clarified. Our study showed that the plasma concentration curve for heme (iron) derived from HbV was similar to that for ^{125}I-HbV and ^{3}H-HbV (Fig. 3). In addition, after an HbV injection, systematic oxidative stress, as estimated by the oxidized albumin ratio, was not increased (data not shown). These results suggest that an excess amount of free heme (iron) derived from HbV was not released in the plasma. In fact, a previous study reported that a daily repeated infusion of HbV (1000 mg of Hb/kg/day) for 14 days had no effect on plasma iron and bilirubin levels. Therefore, phospholipid vesicles for the encapsulation of Hb would be beneficial for heme detoxification through their preferential delivery to the MPS as described in a previous report (Sakai et al., 2004a). Furthermore, deposition of hemosiderin, which is siderosis as heme detoxification, was detected in the liver and spleen after the administration of HbV (2000 mg of Hb/kg), but this deposition completely disappeared after 14 days (Sakai et al., 2001). In the future, it will be necessary to study ferrokinetics to confirm this issue by using Hb with radiolabeled iron (e.g., ^{55}Fe and ^{59}Fe). It will also be interesting to determine whether the deposited iron is effectively used for hematopoiesis after massive blood loss and HbV administration.

Finally, the findings herein show that [^{3}H]cholesterol in HbV was mainly distributed to the liver and spleen, and subsequently excreted into feces approximately 14 days after ^{3}H-HbV injection (Figs. 4 and 5). These results are in good agreement with histopathological examinations, using oil red O staining of liver tissue after an injection of HbV (2000 mg of Hb/kg), which revealed that slight stains were confirmed 3 days after injection and that this staining disappeared within 7 days (Sakai et al., 2001). In addition, Sakai et al. (2004a) found that daily repeated infusion of HbV for 14 days elevated the level of plasma lipid components, one of the risk factors of atherosclerosis, although the effect was temporary. However, cholesterol in the vesicles should reappear in the blood mainly as lipoprotein cholesterol after entrapment in the Kupffer cells and should then be excreted in bile after entrapment of the lipoprotein cholesterol by the hepatocytes (Kuipers et al., 1986). In fact, high levels of radioactivity of ^{3}H in plasma lipoproteins and bile, which are related to carrying and excretion of endogenous cholesterol by physiological pathways, were observed (data not shown). Therefore, it would be desirable to know that cholesterol in the lipid components in HbV behaved the same as endogenous cholesterol after the metabolization of HbV in the MPS.

Conversely, we did not directly examine the disposition of the phospholipid, DPPC, in HbV. Previous reports have shown that phospholipids in the liposome are metabolized in the MPS and reused as cell membranes or are excreted into the bile (Dijkstra et al., 1985; Verkade et al., 1991). Therefore, it is also possible that phospholipids in HbV are metabolized and excreted in the same manner as mentioned above. However, further study will be needed to demonstrate this fact.

Based on the present findings, we propose that the disposition of HbV and its components occurs as follows. After circulating in the form of stable HbV, they are distributed to the liver and spleen, where they are degraded by the MPS. Finally, the enclosed Hb and outer lipid components are eliminated mainly to the urine and feces, respectively, in the same manner as endogenous substances. In addition, our pharmacokinetic study using different animal species enabled us to predict pharmacokinetics in humans. In fact, we reported previously that the half-life of HbV in humans was estimated to be approximately 3 to 4 days by using an allometric equation (Taguchi et al., 2009). The above findings provide further support for the effectiveness and safety of the HbV for use as an oxygen carrier.

References

Abe H, Azuma H, Yamaguchi M, Fujihara M, Ikeda H, Sakai H, Takeoka S, and Tsuchida E (2007) Effects of hemoglobin vesicles, a liposomal artificial oxygen carrier, on hematological responses, complement and anaphylactic reactions in rats. *Artif Cells Blood Substit Immobil Biotechnol* **35**:157–172.

Abe H, Fujihara M, Azuma H, Ikeda H, Ikebuchi K, Takeoka S, Tsuchida E, and Harashima H (2006) Interaction of hemoglobin vesicles, a cellular-type artificial oxygen carrier, with human plasma: effects on coagulation, kallikrein-kinin, and complement systems. *Artif Cells Blood Substit Immobil Biotechnol* **34**:1–10.

Anraku M, Kitamura K, Shinohara A, Adachi M, Suenga A, Maruyama T, Miyanaka K, Miyoshi T, Shiraishi N, Nonoguchi H, et al. (2004) Intravenous iron administration induces oxidation of serum albumin in hemodialysis patients. *Kidney Int* **66**:841–848.

Anraku M, Kitamura K, Shintomo R, Takeuchi K, Ikeda H, Nagano J, Ko T, Mera K, Tomita K, and Otagiri M (2008) Effect of intravenous iron administration frequency on AOPP and inflammatory biomarkers in chronic hemodialysis patients: a pilot study. *Clin Biochem* **41**:1168–1174.

Balla J, Vercellotti GM, Jeney V, Yachie A, Varga Z, Eaton JW, and Balla G (2005) Heme, heme oxygenase and ferritin in vascular endothelial cell injury. *Mol Nutr Food Res* **49**:1030–1043.

Buehler PW and Alayash AI (2004) Toxicities of hemoglobin solutions: in search of in-vitro and in-vivo model systems. *Transfusion* **44**:1516–1530.

Burger AG, Engler D, Buergi U, Weissel M, Steiger G, Ingbar SH, Rosin RE, and Babior BM (1983) Ether link cleavage is the major pathway of iodothyronine metabolism in the phagocytosing human leukocyte and also occurs in vivo in the rat. *J Clin Invest* **71**:935–949.
Cabrales P, Sakai H, Tsai AG, Takeoka S, Tsuchida E, and Intaglietta M (2005) Oxygen transport by low and normal oxygen affinity hemoglobin vesicles in extreme hemodilution. *Am J Physiol Heart Circ Physiol* **288**:H1885–H1892.
Dijkstra J, van Galen M, Regts D, and Scherphof G (1985) Uptake and processing of liposomal phospholipids by Kupffer cells in vitro. *Eur J Biochem* **148**:391–397.
Goda N, Suzuki K, Naito M, Takeoka S, Tsuchida E, Ishimura Y, Tamatani T, and Suematsu M (1998) Distribution of heme oxygenase isoforms in rat liver: topographic basis for carbon monoxide-mediated microvascular relaxation. *J Clin Invest* **101**:604–612.
Gröne EF and Gröne HJ (2008) Does hyperlipidemia injure the kidney? *Nat Clin Pract Nephrol* **4**:424–425.
Izumi Y, Sakai H, Hamada K, Takeoka S, Yamahata T, Kato R, Nishide H, Tsuchida E, and Kobayashi K (1996) Physiologic responses to exchange transfusion with hemoglobin vesicles as an artificial oxygen carrier in anesthetized rats: changes in mean arterial pressure and renal cortical tissue oxygen tension. *Crit Care Med* **24**:1869–1873.
Kadowaki D, Anraku M, Tasaki Y, Kitamura K, Wakamatsu S, Tomita K, Gebicki JM, Maruyama T, and Otagiri M (2007) Effect of olmesartan on oxidative stress in hemodialysis patients. *Hypertens Res* **30**:395–402.
Keipert PE (1995) Use of Oxygent, a perfluorochemical-based oxygen carrier, as an alternative to intraoperative blood transfusion. *Artif Cells Blood Substit Immobil Biotechnol* **23**:381–394.
Kiwada H, Matsuo H, and Harashima H (1998) Identification of proteins mediating clearance of liposomes using a liver perfusion system. *Adv Drug Deliv Rev* **32**:61–79.
Kristiansen M, Graversen JH, Jacobsen C, Sonne O, Hoffman HJ, Law SK, and Moestrup SK (2001) Identification of the haemoglobin scavenger receptor. *Nature* **409**:198–201.
Kuipers F, Spanjer HH, Havinga R, Scherphof GL, and Vonk RJ (1986) Lipoproteins and liposomes as in vivo cholesterol vehicles in the rat: preferential use of cholesterol carried by small unilamellar liposomes for the formation of muricholic acids. *Biochim Biophys Acta* **876**:559–566.
Murata M, Tamai I, Sai Y, Nagata O, Kato H, Sugiyama Y, and Tsuji A (1998) Hepatobiliary transport kinetics of HSR-903, a new quinolone antibacterial agent. *Drug Metab Dispos* **26**:1113–1119.
Nakajou K, Horiuchi S, Sakai M, Hirata K, Tanaka M, Takeya M, Kai T, and Otagiri M (2005) CD36 is not involved in scavenger receptor-mediated endocytic uptake of glycolaldehyde- and methylglyoxal-modified proteins by liver endothelial cells. *J Biochem* **137**:607–616.
Nosé Y (2004) Is there a role for blood substitutes in civilian medicine: a drug for emergency shock cases? *Artif Organs* **28**:807–812.
Sakai H, Hara H, Yuasa M, Tsai AG, Takeoka S, Tsuchida E, and Intaglietta M (2000a) Molecular dimensions of Hb-based O_2 carriers determine constriction of resistance arteries and hypertension. *Am J Physiol Heart Circ Physiol* **279**:H908–H915.
Sakai H, Horinouchi H, Tomiyama K, Ikeda E, Takeoka S, Kobayashi K, and Tsuchida E (2001) Hemoglobin-vesicles as oxygen carriers: influence on phagocytic activity and histopathological changes in reticuloendothelial system. *Am J Pathol* **159**:1079–1088.
Sakai H, Masada Y, Horinouchi H, Ikeda E, Sou K, Takeoka S, Suematsu M, Takaori M, Kobayashi K, and Tsuchida E (2004a) Physiological capacity of the reticuloendothelial system for the degradation of hemoglobin vesicles (artificial oxygen carriers) after massive intravenous doses by daily repeated infusions for 14 days. *J Pharmacol Exp Ther* **311**:874–884.
Sakai H, Masada Y, Horinouchi H, Yamamoto M, Ikeda E, Takeoka S, Kobayashi K, and Tsuchida E (2004b) Hemoglobin-vesicles suspended in recombinant human serum albumin for resuscitation from hemorrhagic shock in anesthetized rats. *Crit Care Med* **32**:539–545.
Sakai H, Seishi Y, Obata Y, Takeoka S, Horinouichi H, Tsuchida E, and Kobayashi K (2009) Fluid resuscitation with artificial oxygen carriers in hemorrhaged rats: profiles of hemoglobin-vesicle degradation and hematopoiesis for 14 days. *Shock* **31**:192–200.
Sakai H, Sou K, Horinouchi H, Kobayashi K, and Tsuchida E (2008) Haemoglobin-vesicles as artificial oxygen carriers: present situation and future visions. *J Intern Med* **263**:4–15.
Sakai H, Takeoka S, Park SI, Kose T, Nishide H, Izumi Y, Yoshizu A, Kobayashi K, and Tsuchida E (1997) Surface modification of hemoglobin vesicles with poly(ethylene glycol) and effects on aggregation, viscosity, and blood flow during 90% exchange transfusion in anesthetized rats. *Bioconjug Chem* **8**:23–30.
Sakai H, Takeoka S, Yokohama H, Seino Y, Nishide H, and Tsuchida E (1993) Purification of concentrated hemoglobin using organic solvent and heat treatment. *Protein Expr Purif* **4**:563–569.
Sakai H, Tomiyama KI, Sou K, Takeoka S, and Tsuchida E (2000b) Poly(ethylene glycol)-conjugation and deoxygenation enable long-term preservation of hemoglobin-vesicles as oxygen carriers in a liquid state. *Bioconjug Chem* **11**:425–432.
Sakai H, Yuasa M, Onuma H, Takeoka S, and Tsuchida E (2000c) Synthesis and physicochemical characterization of a series of hemoglobin-based oxygen carriers: objective comparison between cellular and acellular types. *Bioconjug Chem* **11**:56–64.
Savitsky JP, Doczi J, Black J, and Arnold JD (1978) A clinical safety trial of stroma-free hemoglobin. *Clin Pharmacol Ther* **23**:73–80.
Shimoishi K, Anraku M, Kitamura K, Tasaki Y, Taguchi K, Hashimoto M, Fukunaga E, Maruyama T, and Otagiri M (2007) An oral adsorbent, AST-120 protects against the progression of oxidative stress by reducing the accumulation of indoxyl sulfate in the systemic circulation in renal failure. *Pharm Res* **24**:1283–1289.
Sou K, Klipper R, Goins B, Tsuchida E, and Phillips WT (2005) Circulation kinetics and organ distribution of Hb-vesicles developed as a red blood cell substitute. *J Pharmacol Exp Ther* **312**:702–709.
Taguchi K, Maruyama T, Iwao Y, Sakai H, Kobayashi K, Horinouchi H, Tsuchida E, Kai T, and Otagiri M (2009) Pharmacokinetics of single and repeated injection of hemoglobin-vesicles in hemorrhagic shock rat model. *J Control Release* doi: 10.1016/j.jconrel.2009.02.009.
Verkade HJ, Derksen JT, Gerding A, Scherphof GL, Vonk RJ, and Kuipers F (1991) Differential hepatic processing and biliary secretion of head-group and acyl chains of liposomal phosphatidylcholines. *Biochem J* **275 (Pt 1)**:139–144.
Winslow RM (2005) Targeted O_2 delivery by low-p50 hemoglobin: a new basis for hemoglobin-based oxygen carriers. *Artif Cells Blood Substit Immobil Biotechnol* **33**:1–12.
Yamaoka K, Tanigawara Y, Nakagawa T, and Uno T (1981) A pharmacokinetic analysis program (multi) for microcomputer. *J Pharmacobiodyn* **4**:879–885.
Yu B, Raher MJ, Volpato GP, Bloch KD, Ichinose F, and Zapol WM (2008) Inhaled nitric oxide enables artificial blood transfusion without hypertension. *Circulation* **117**:1982–1990.

Address correspondence to: Dr. Masaki Otagiri, Department of Biopharmaceutics, Graduate School of Pharmaceutical Sciences, Kumamoto University, 5-1 Oe-honmachi, Kumamoto 862-0973, Japan. E-mail: otagirim@gpo.kumamoto-u.ac.jp

Histopathological changes of rat brain after direct injection of Hb-vesicles (artificial oxygen carriers) and neurological impact in an intracerebral hemorrhage model

Hiromi Sakai,[1] Michiko Okamoto,[2] Eiji Ikeda,[3] Hirohisa Horinouchi,[4] Koichi Kobayashi,[4] Eishun Tsuchida[1]
[1]*Research Institute for Science and Engineering, Waseda University, Tokyo 169-8555, Japan*
[2]*Department of Pharmacology, Weill Medical College of Cornell University, New York 10021*
[3]*Department of Pathology, School of Medicine, Keio University, Tokyo 160-8582, Japan*
[4]*Department of General Thoracic Surgery, School of Medicine, Keio University, Tokyo 160-8582, Japan*

Received 17 December 2007; revised 9 May 2008; accepted 20 May 2008
Published online 31 July 2008 in Wiley InterScience (www.interscience.wiley.com). DOI: 10.1002/jbm.a.32164

Abstract: For use as artificial oxygen carriers during transfusion, the safety and efficacy of Hb-vesicles (HbV, 250 nm), have been investigated extensively. Nevertheless, their neurotoxicity remains unknown. We explored potential adverse effects of HbV in the brain using a rat intracerebral hemorrhage model. Male Wistar rats were anesthetized with sevoflurane and fixed on a stereotaxic frame. Then HbV or homologous RBC suspension ([Hb] = 8.6 g/dL, 20 μL) was injected into the right caudate nucleus. All animals survived, gained weight, and maintained their well-being until the time of sacrifice; except during the first few days after surgery. However, both groups showed slight weakness in hind leg retraction, occasional ataxia/gait, and piloerection. Neutrophils accumulated at the onset of injury in perihematomal tissues in both groups at 1st day, but had disappeared by 3 days. Infiltration of small HbV in the perihematomal tissue was prominent at 1st day; phagocytized HbV were detected in macrophages. Hemeoxygenase-1 and hemosiderin deposition appeared after 3 days, reflecting the degradation of both HbV and RBC. The HbVs were detectable even after 28 days in the HbV group, but no residual RBCs were detected in the RBC group. Both groups showed proliferation of astrocytes, named gliosis, for tissue reconstruction after 3 days. This study revealed no notable differences in adverse effects between the intra-cerebral injection of HbV and the RBC control on behavioral functions and brain tissue responses. © 2008 Wiley Periodicals, Inc. J Biomed Mater Res 90A: 1107–1119, 2009

Key words: artificial oxygen carriers; blood substitutes; liposome; intracerebral hemorrhage; neurotoxicity

INTRODUCTION

For possible use as a transfusion alternative, Hb-vesicles (HbV), or liposome-encapsulated Hb, were developed as artificial oxygen carriers.[1–5] The HbV safety and efficacy have been studied extensively in our laboratory. HbV is void of blood-type antigens and blood-borne pathogens, and can be stored for at least 2 years at room temperature.[6–8] The cellular structure and HbV particles are sufficiently large to prevent extravasation across the hepatic fenestrated endothelium, so as not to modulate the reaction with endogenous NO and CO as vasorelaxation factors.[9–11] The fate of HbV after oxygen transport is accumulation and prompt degradation in the reticuloendothelial system, primarily by spleen macrophages and liver Kupffer cells, and similar to that of senescent RBCs. The circulation time, however, was shorter for HbV than for RBC.[5,12–14]

It is known from clinical information that hemorrhagic shock and resuscitation often produce brain damage from the opening of blood brain barrier (BBB), and infiltration of blood components into the brain tissue, leading to tissue inflammation and neuronal cell death.[15] However, HbV would not infiltrate through the BBB because of its vesicular size, which is 250 nm on average, is considerably larger than that of any other plasma proteins. We further investigated possible HbV neurotoxic effects by direct injection of HbV into the rat brain compartment. When the BBB is damaged by a traumatic injury or an intracerebral hemorrhage (ICH) and when blood is infiltrated into the brain, the process

Correspondence to: E. Tsuchida; e-mail: hiromi@waseda.jp; eishun@waseda.jp

induces local inflammation and migration of immuno-protective cells such as microglia. In patients suffering from brain hemorrhage or stroke, the released Hb by breakdown of RBC and its byproducts such as iron are known to produce neuronal damage.[16–18] HbV encapsulates purified Hb solution in phospholipid vesicles. Therefore, an equivalent neurotoxicity of RBC might be expected from the released Hb and its byproducts when the HbVs break down. However, because the chemical composition and the stability of HbV lipid membrane differ from those of RBCs, the HbV breakdown process might produce quantitatively different neurotoxicity. In 2004, the FDA listed eight unsolved safety-related problems of Hb-based oxygen carriers. One was neurotoxicity because it is anticipated that Hb, entering the brain from the vasculature, can cause considerable tissue damage, engendering disability or morbidity.[19,20]

Given this background, the current study tested the possible neurotoxic effect of HbV comparative to that of RBC, when it is injected directly into the brain compartment. For the purpose, HbV was injected into basal ganglia on one side and the neurotoxic effects were examined using pathological procedures and using histochemical and immunohistochemical methods. Their consequent behavior responses were also studied.

MATERIALS AND METHODS

Preparation of Hb-vesicles

HbVs were prepared by Oxygenix Co. (Tokyo, Japan) as reported previously.[6,7,21,22] The Hb was purified from outdated and donated blood provided by the Japanese Red Cross Society (Tokyo, Japan). The encapsulated Hb (38 g/dL) contained 14.7 m*M* pyridoxal 5′-phosphate (PLP; Sigma-Aldrich Corp., St. Louis, MO) as an allosteric effector at a molar ratio of PLP/Hb = 2.5. The lipid bilayer comprised 1,2-dipalmitoyl-*sn*-glycero-3-phosphatidylcholine, cholesterol, 1,5-*O*-dihexadecyl-*N*-succinyl-L-glutamate (Nippon Fine Chemical Co., Osaka, Japan), and 1,2-distearoyl-*sn*-glycero-3-phosphatidyethanolamine-*N*-PEG_{5000} (NOF Corp., Tokyo, Japan) at a molar composition of 5/5/1/0.033. The lipopolysaccharide content, measured using a modified *Limulus* amebocyte lysate test, was <0.2 EU/mL.[23] The physicochemical characteristics of HbVs are P_{50}, 25 Torr, 251 ± 81 nm particle diameter, and < 3% MetHb. Prior to use, HbV suspended in saline (0.9% sodium chloride; [Hb] = 10 g/dL, 8.6 mL) was mixed with recombinant human serum albumin (rHSA, 25 g/dL, 1.4 mL; Nipro Corp., Osaka, Japan), making the final rHSA concentration in the suspending medium 5 g/dL; this caused the final Hb concentration to 8.6 g/dL.[4,5] At this condition, the colloid osmotic pressure (COP) and the viscosity (300 s^{-1}, 37°C) of the HbV/rHSA were, respectively, 20 mmHg and 2.9 cP.

Preparation of washed rat RBC

Blood was withdrawn from the anesthetized donor Wistar rats via the caudal vena cava into a heparinized syringe. The blood was centrifuged for 10 min at 4000 × *g*; the supernatant and the buffy coat were removed. The sedimented RBCs were re-suspended in saline and centrifuged. This procedure was repeated twice. The RBCs were suspended finally in a 5 g/dL rHSA solution. The final Hb concentration in the suspension was made to 8.6 g/dL and to the same Hb concentration as that in the HbV suspension.

Injection of the sample solution into brain tissue

The experimental protocol was fully approved by the Institute of Laboratory Animal Care and Use Committee, Keio University School of Medicine. Relevant NIH guidelines (NIH Publication no. 85-23 Rev. 1985) were observed. All survival surgical procedures were performed under the Institutional Animal and Use Committee guideline. In all, 69 male Wistar rats were used for this study (Sankyo Labo Service Co., Tokyo, Japan). Each animal was placed in a gas-tight glass jar; the anesthesia was induced with ether. The animal was then mounted to a small animal standard stereotaxic frame (Kent Scientific Corp., Torrington, CT). The surgical anesthesia was maintained with 1.3–1.5% sevoflurane (Maruishi Pharm., Co., Osaka, Japan) delivered through a flow regulated gas anesthetic machine (Model TK-4 Biomachinery; Kimura Medical Instrument Co., Tokyo, Japan) and through a nose cone attached to the stereotaxic frame and to the animal. Body temperatures of the animals were maintained at 37°C throughout the surgery using a heating pad. Each animal's head was shaven; the skin was disinfected with 70% ethanol and Isozin, and a local anesthetic, bupivacaine hydrochloride (0.25%; Marcain^{R} injection; AstraZeneca, Osaka, Japan) before making an incision. The skull was exposed by midline incision; underlying muscle layers were retracted to expose the bone surface. Lambda was identified. The injection site was at the basal ganglia area, marked according to the rat stereotaxic map coordinate of 2.4 mm anterior to lambda, 4 mm lateral to midline, and 5 mm ventral from the surface. A hole was drilled through the skull bone on right side.

The testing solution (either one of HbV or RBC), 20 μL, was injected at a rate of 4 μL/min through the 28-G needle attached to Hamilton micro-syringe; the needle was held in place for 3 min after the completion of injection (HbV, n = 34; RBC, n = 28). The needle site was plugged with Gelform (Pharmacia and Upjohn, Kalamazoo, MI) to prevent cerebrospinal fluid leak; the hole of the skull was sealed with dental cement (Ionotite; Tokuyama Dental Co., Tokyo, Japan). The skin was closed with either wound clips or an absorbable suture. An antibiotic, Cefmetazole sodium, 20 mg/kg SC (Sankyo Pharmaceutical, Tokyo), and an opioid analgesic, Buprenorphine hydrochloride (Lepetan injection; Otsuka Pharm., Tokyo, Japan), 0.05 mg/kg, SC, were given after the surgery. The animal was kept on a temperature-controlled bed in a cage and observed until

full recovery from the anesthesia. The animals were then housed in cages and provided with food and water *ad libitum* in a temperature-controlled room with a 12-h dark/light cycle. The animals were observed at 6-, 12-, and 24-h post-surgery for any sign of bleeding from the site of incision, as well as pain and discomfort and infection. The well-being of animals was followed daily throughout the experiment. Buprenorphine injections were repeated every 8 h if there was any sign of pain or discomfort.

Behavioral testing

Body weights of animals and their well-being were observed at 1, 2, 3, 5, 14, and 28 days after the surgery and prior to the time of sacrifice for histopathological studies. Similarly, behavioral testing, which indicated motor dysfunction, was performed on the days presented in Table I. Data of the normal rat group (no treatment, $n = 7$) were also collected.

Histopathological examination

At 1, 3, 7, and 28 days after the surgery, seven animals in each group were euthanized with ether in a gas chamber. The brain was isolated; its wet weight was measured. The brain was then fixed in a 10% formalin-phosphate buffer solution (Wako Pure Chemical Industries, Tokyo, Japan). The fixed brain was sliced to 1-mm thickness, anterior and posterior, vertical to the injection needle mark.

The sliced brain was examined histochemically using hematoxylin and eosin (HE) staining for any pathological changes, and Berlin blue staining to confirm the presence of hemosiderin. Immunohistochemical stains were performed for glial fibrillary acidic protein (GFAP) of astrocytes, inducible hemoxygenase-1 (HO-1), human Hb of HbV, and apoptotic cells.

For immunohistochemistry to observe astrocytes, the paraffin sections (4-μm thick) were mounted on 3-aminoprophyl triethoxysilane-coated glasses. After deparaffinization, the sections were subjected to microwave treatment for 10 min with 10 m*M* citrate buffer (pH 6.0) for antigen retrieval. They were incubated with methanol containing 0.3% hydrogen peroxide (H_2O_2) for 30 min at room temperature, and subsequently with 2.5% normal horse serum for 15 min at room temperature. The tissues were then reacted with mouse monoclonal antibody against GFAP (1/200 dilution; Dako, Glostrup, Denmark) for 3 h at room temperature. After washing in PBS, they were incubated in ImmPress Reagent Peroxidase anti-mouse Ig (ImmPress Reagent Kit; Vector Laboratories, CA) for 1 h at room temperature. The color was developed with 3,3′-diaminobenzidine tetrahydrochloride (DAB, 0.2 mg/mL; Dojindo Laboratories, Kumamoto, Japan) in 0.05 *M* Tris-HCl (pH 7.6) containing 0.003% H_2O_2; the tissues were then counterstained with hematoxylin.

The staining methods of anti-rat HO-1 and anti-human Hb antibody have been described previously.[13,14] Briefly, the sections were treated with proteinase K (Dako, Glostup, Denmark) for antigen retrieval. After blocking the nonspecific binding with DAKO Antibody Diluent Solu-

TABLE I
Daily Behavioral Testing After Direct Injection of the Sample Solutions into the Brain

	Circling Behavior[a] (%)			Piloerection[b] (%)			Hind Leg Weakness[c] (%)			Absence of Startle Response[d] (%)			Hanging Time[e] (s)		
Days	Normal Rat	HbV	RBC	Normal Rat	HbV	RBC	Normal Rat	HbV	RBC	Normal Rat	IIbV	RBC	Normal Rat	IIbV	RBC
1	0	0	0	71	41	25	14	71	78	0	23	13	18 ± 3	10 ± 1*	9 ± 1*
2	0	0	0	29	30	43	14	63	86	0	11	15	15 ± 4	12 ± 1	10 ± 1
3	0	0	0	29	61	53	29	56	62	0	26	23	14 ± 3	15 ± 2	11 ± 1
5	0	0	0	43	60	70	14	44	36	0	7	20	16 ± 4	17 ± 2	11 ± 2
7	0	0	0	29	33	70	29	33	21	0	13	0	13 ± 2	16 ± 3	12 ± 3
14	0	0	0	14	36	57	14	50	57	0	0	0	13 ± 4	13 ± 2	8 ± 2
28	0	0	0	43	50	86	29	75	100	0	0	0	5 ± 1	9 ± 2	9 ± 2

The number of animals (n) at each day: HbV group, 1d (34), 2d (27), 3d (23), 5d(15), 7d (15), 14d (11), and 28d (8); RBC group, 1d (28), 2d (21), 3d (17), 5d (10), 7d (10), 14d (7), and 28d (7); the normal rat group (no treatment), 1d – 28d (7).

[a]Spontaneous body circling.

[b]Ruffling of the body hair.

[c]Hesitant to walk on the beam (1.5 cm wide), and misses steps often; drags the foot as a rat walks on the beam.

[d]Startles and jumps to the blow of air to the face.

[e]Length of time spent hanging in second on a round plastic rod, diameter 4 mm. Mean ± SE.

*$p < 0.05$ vs. the normal rat group.

tion, they were incubated with mouse monoclonal antibody against rat HO-1 (GTS-3; Takara, Tokyo, Japan). They were then incubated with the secondary antibody (Simple Stain Rat MAX-PO[M]); Nichirei Corp., Tokyo, Japan). The color was developed using DAB, and the sections were counterstained with hematoxylin. A comparative staining procedure was performed with non-immune mouse IgG to confirm that the staining was specific to HO-1 and not derived from the color of hemosiderin deposition (DAKO).

For detection of human Hb derived from HbV, the sections were treated with rabbit polyclonal antibodies against human Hb (Dako). They were further incubated with alkaline phosphatase-conjugated swine antibodies against rabbit immunoglobulins (Dako)). The color was then developed using a New Fuchsin Substrate Kit (Nichirei Corp., Tokyo, Japan); the sections were counterstained with hematoxylin.

Apoptotic cells were stained with terminal deoxynucleotidyl transferase dUTP Nic-end labeling (TUNEL) with ApopTag^R Peroxidase *In Situ* Apoptosis Detection Kit (Chemicon International, Temecula, CA). The detailed protocol is described in the kit operating instruction. After pretreatments for antigen retrieval and quenching of endogenous peroxidase, the sections were incubated with a terminal deoxynucleotidyl transferase (TdT) enzyme solution, followed by a solution of anti-digoxigenin conjugate. The color was developed with peroxidase substrate and counterstained with hematoxylin.

Transmission electron microscopic observation (TEM) was performed to visualize the presence of the HbV particles in the brain tissue (PCL Japan, Tokyo, Japan). One brain of the HbV group at 1, 3, 7, and 28 days was fixed with 2.5% glutaraldehyde solution, cut in ~2-mm^3 blocks, and stored in 8% sucrose solution (0.1 mol/L phosphate buffer, pH 7.4). The fixed blocks were then washed with 0.1 mL/L phosphate buffer and stained with 2% osmic acid solution at 4°C for 2 h. Next, the blocks were dehydrated with ethanol solution by a stepwise increase in ethanol concentrations (50, 60, 70, 80, 90, 95, and 100%), 10 min for each step, washed with propylene oxide; then polymerized using Quetol 812 at 60°C for 28 h. The obtained blocks were sliced into 60–70 nm thickness using an Ultracut S microtome. The sliced tissues were stained with 3% uranyl acetate solution for 16–20 min, then treated with Satoh's lead solution (lead acetate, lead nitrate, and lead citrate) in citrate for 5 min, washed, and dried. The sliced brain tissues were examined under a transmission electron microscope (TEM, JEM-100CX; JEOL, Tokyo, Japan) and photographed.

Data analysis

The *in vivo* data are presented as mean ± SE with the indicated number of animals tested. Unpaired *t*-tests were used to compare the HbV and RBC groups.

In vitro stability of Hb-vesicles and RBC

Degradation rate of HbV would be influenced by the stability of HbV vesicles withstanding physical stimuli and enzymatic attack. To collect some information related to stability, the following three sets of *in vitro* experiments were performed:

1. Hypotonic hemolysis was induced by mixing HbV or RBC suspensions with distilled water at a 1:4 volume ratio ([Hb] = 1.72 g/dL). The mixture was then centrifuged and the supernatant Hb concentration was measured using a cyanomethemoglobin method[24] to determine the percentage of hemolysis.
2. Resistance of hemolysis to freeze-thawing was tested by diluting the sample of HbV or RBC 10 times with saline solution ([Hb] = 1.72 g/dL). One milliliter of the sample was put in a plastic tube and dipped in liquid-nitrogen for a few minutes. It was then thawed at room temperature. The samples were centrifuged and the supernatant Hb concentration was determined by the same method.
3. Hemolysis was induced by the enzymatic attack with phospholipase A_2 (PLA_2) to membrane phospholipids.[25] Four hundreds microliters of sample solutions of HbV or RBC in PBS ([Hb] = 1.6 g/L, pH 7.2) was added to a 400 μL stock solution of 10 m*M* $CaCl_2$ and 3 μg/mL PLA_2 (from Naja mossambica mossambica; Sigma, MO). The mixture was incubated for 0.5 and 2 h at 37°C; EDTA was then added to make a final concentration of 2 m*M*; the tube was cooled in ice for 5 min. The testing solutions were centrifuged or ultracentrifuged, and the supernatant was determined for Hb concentration to calculate the degree of hemolysis. The data are expressed as mean ± SE.

RESULTS

Body weight and behavioral testing

All animals in both HbV/rHSA and RBC/rHSA groups survived. After a slight weight reduction during the first 3 days, their body weights increased steadily to 327 ± 3 g at 28 days after the treatment (Fig. 1). Because of the initial loss, both groups showed lighter body weights in comparison to the normal rat group (untreated). The wet brain weight for both groups increased along with the increasing body weight (on the average HbV group, from 1.84 ± 0.04 to 1.94 ± 0.02 g; RBC group, from 1.86 ± 0.02 to 1.97 ± 0.02 g). No significant difference was apparent between the HbV and the RBC treated groups in brain weights.

The results of behavioral testing (Table I) indicate that animals in both HbV and RBC treated groups displayed no overt circling movement. Piloerection and startle responses were apparent for both groups; however, the startle responses reverted to normal by 7 days in both groups. The testing of the hind leg weakness on the beam showed signs of disability, that is, miss-steps and dragging of the left foot, in both treated groups; they were observed more often than in the untreated rat group. The testing of the

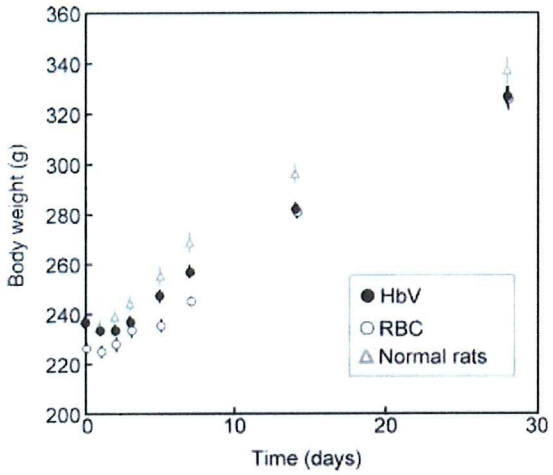

Figure 1. Changes in body weight after intracerebral injection of HbV or RBC. A slight reduction of body weight was apparent for 3 days at the beginning in both groups. However, the rats grew and gained weight rapidly to about 330 g at 28 days. Mean ± SE. Data of normal rats (no treatment) were also plotted as a reference.

ability to hang on a bar with front paws, which was the most sensitive test to detect the lack of motor coordination in our behavioral testing measures, showed some reduction in hanging time (HbV, 10 ± 1 s vs. RBC, 9 ± 1 s), with a significant difference from the untreated group (18 ± 3 s); however, no significant difference was found after 2 days until 28 days.

Histopathological examination of brain

The tip of the needle was positioned to the area of basal ganglia (Fig. 2). One day after the injection, HE staining showed the presence of hematoma in both groups. The HbV group showed a spread of red coloration in the perihematomal region, indicating that small HbV infiltrated into the surrounding parenchyma tissue. In the HbV group, the hematoma was composed of injected HbV and autologous blood because of bleeding caused by the needle insertion. A magnified photograph showed the presence of neutrophils surrounding the hematoma in both HbV and RBC groups because of the inflammatory reaction. The quantities of neutrophils were highest 1 day after injection in both groups; the numbers decreased significantly by 3 days. No notable difference in cellular responses was found between the two groups.

Staining with anti-human Hb antibody also supported the fact that HbV were diffused into the parenchyma. It was inferred from the micrographs taken 1, 3, and 28 days after the HbV injection (Fig. 3) that HbV was phagocytized by macrophages. The number of such macrophages decreased markedly by 28 days. However, the micrograph clearly showed the presence of human Hb in HbV, even after 28 days. Correspondingly, TEM clearly showed the presence of HbV in the phagosomes of macrophages at 1 and 3 days (Fig. 4). A macrophage phagocytizing both HbV and RBC is apparent as shown in the HbV group.

Staining with anti HO-1 antibody showed the induction of HO-1 at 3 and 7 days after injection for both HbV and RBC groups, particularly at the rim of the hematoma region (Fig. 5). However, the macrophages stained with HO-1 in the HbV group appeared more widely distributed in the perihematoma region compared with the RBC group at 28 days (data not shown). The DAB staining procedure with non-immune IgG instead of anti HO-1 antibody showed no brown staining (data not shown). It is concluded, therefore, that the brown stains are specific to HO-1 and not derived from hemosiderin.

Berlin blue method confirmed the hemosiderin deposition from 3 days after injection. A large amount of hemosiderin was deposited at a nearby hematoma site in both groups at 7 days (Fig. 6). The tissue area containing the HbV, however, showed less hemosiderin deposition. At 28 days, the hemosiderin remained in both groups.

Regarding immunochemical studies with GFAP, the reactive proliferation of astrocytes and gliosis was detectable at 3 days in both groups (Fig. 7). The hypertrophic and hyperplastic astrocytes were distributed in the area of the hematoma. The reconstruction processes were seen to occur by scar tissue formation, namely gliosis. Astrocytic cell reaction progressed. The glial fibers became stouter and more numerous, showing fibrillary gliosis at 28 days in both groups.

Furthermore, TUNEL-staining clarified the presence of apoptotic cells surrounding the hematoma in both groups. The HbV group showed 4.3 ± 3.6 cells (1 day), 2.0 ± 0.4 cells (3 days), 8.0 ± 1.9 cells (7 days), and 13.2 ± 4.1 cells (28 days). The RBC group showed 11.9 ± 7.2 cells (1 day), 1.5 ± 0.7 cells (3 days), 20.4 ± 9.8 cells (7 days), and 19.0 ± 6.1 cells (28 days). Both groups showed considerable variation in number of apoptotic cells. However, the RBC group displayed a greater number of apoptotic cells overall than in the HbV group, especially at 7 days.

In vitro stability of Hb-vesicles and RBC

Hypotonic challenge induced 94% hemolysis for rat RBC, although HbV showed essentially no hemolysis (Table II). Freezing of water, crystallization of bulk water molecules, facilitates dehydration of the surface of lipid membranes, and destroys the cellular structure. Freeze-thawing induced 78% hemolysis for

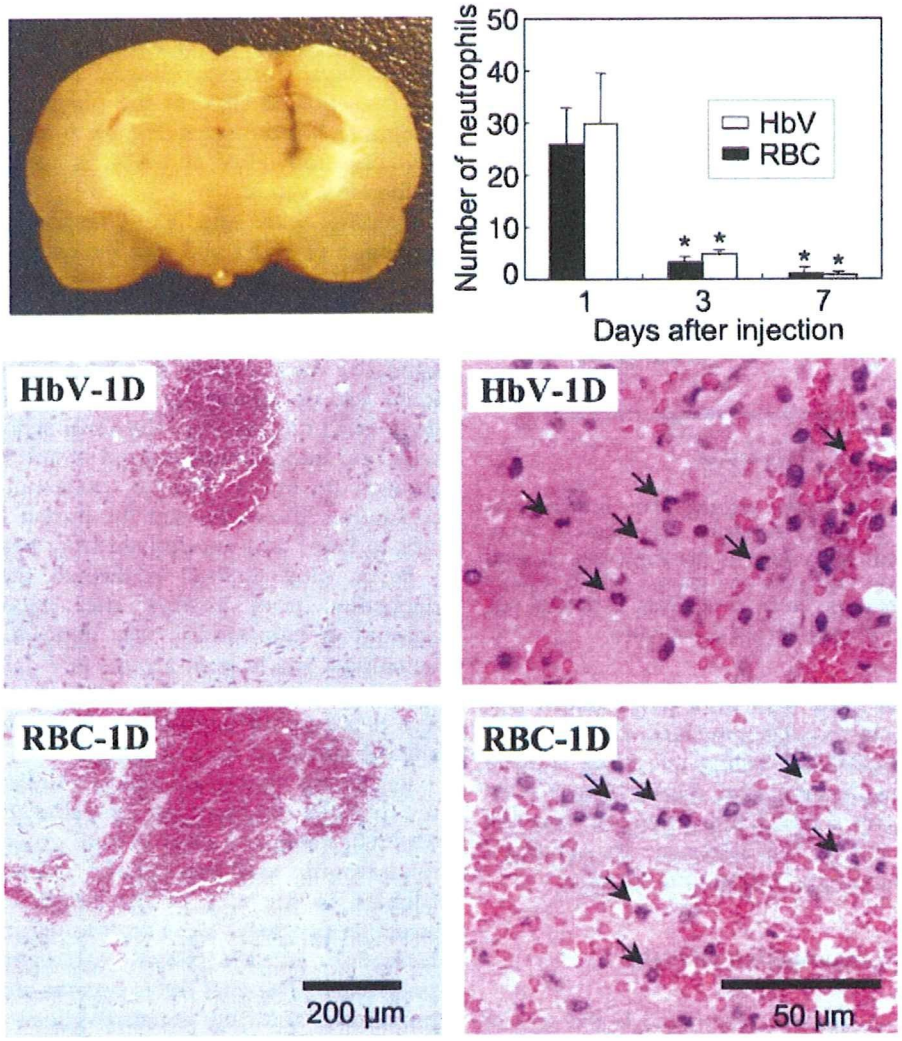

Figure 2. (Left Top) The needle tip for the intracerebral injection reached to the caudate nucleus. (Left middle, bottom) Hematoxylin/eosin staining of rat brain showing the presence of hematoma 1 day after injection. The HbV group showed the red area in the parenchymal region, indicating the presence of dispersed HbV. The RBC group showed that most of the RBCs remained in the hematoma. (Right, middle, and bottom) Hematoxylin/eosin staining of rat brain showing the presence of neutrophils (indicated with arrows) surrounding the hematoma in both HbV and RBC groups 1 day after injection because of the inflammatory reactions. (Right top) The quantities of neutrophils (in 0.26 mm^2) were greatest 1 day after injection. Then they decreased significantly 3 days after injection ($*p < 0.05$ vs. 1 day). However, no differences were found between any of the HbV with the RBC groups. [Color figure can be viewed in the online issue, which is available at www.interscience.wiley.com.]

RBC whereas HbV showed only 20% hemolysis. HbV was resistant to the attack of PLA_2. Hemolysis was almost not induced in the HbV sample, whereas RBC showed 18% hemolysis.

DISCUSSION

The main finding of this study is that the intracerebral injection of 20 μL HbV showed normal progression of pathological responses to ICH. No difference was evident between HbV and RBC injections in the conventional rat ICH model, except that HbV distributed more widely in the perihematomal tissue and that a slight amount of HbV remained even after 28 days.

A clinical application of Hb-based oxygen carriers (HBOCs) can be a resuscitative fluid, which can be used for traumatic hemorrhaged patients.[26] However, most conventional experimental animal models have tested the effectiveness of HBOCs on artificially created hemorrhagic conditions that do not involve

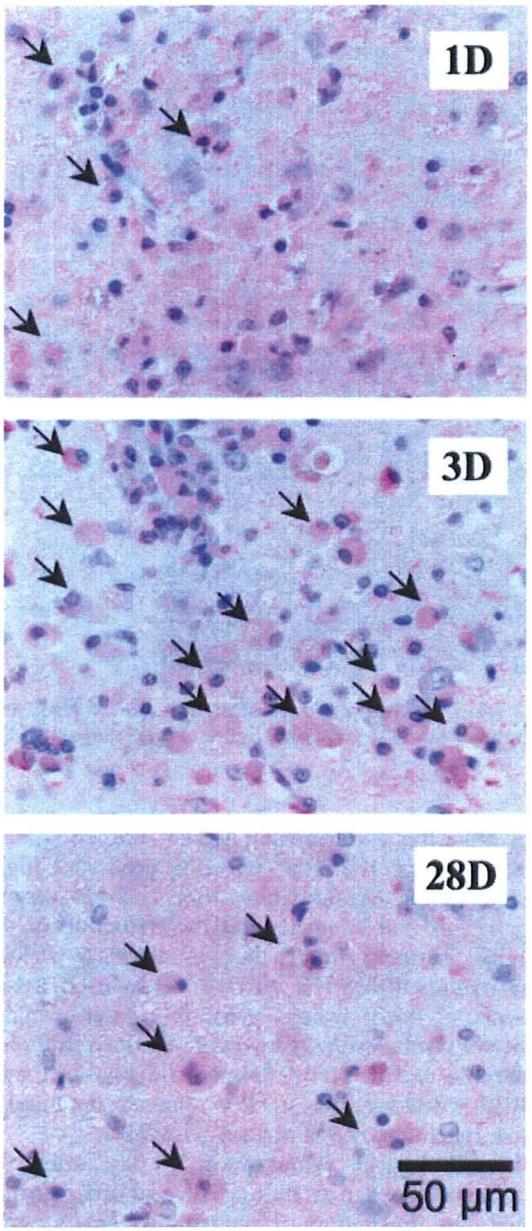

Figure 3. Immunochemical staining of rat brain tissue near the hematoma with anti-human Hb antibody. The round pink cells indicate the presence of HbV inside the cells. One day and three days after injection, the macrophages phagocytizing HbV are evident, as indicated with arrows. Even after 28 days, a large amount of HbV remained, although such cells were markedly fewer. [Color figure can be viewed in the online issue, which is available at www.interscience.wiley.com.]

head injury.[4,27,28] Therefore, it is important to test possible adverse effects of HBOC when it is used for treatment of trauma such as in head injury involving brain hemorrhage.[20] Accordingly, examining the effects of HbV through a direct injection into the

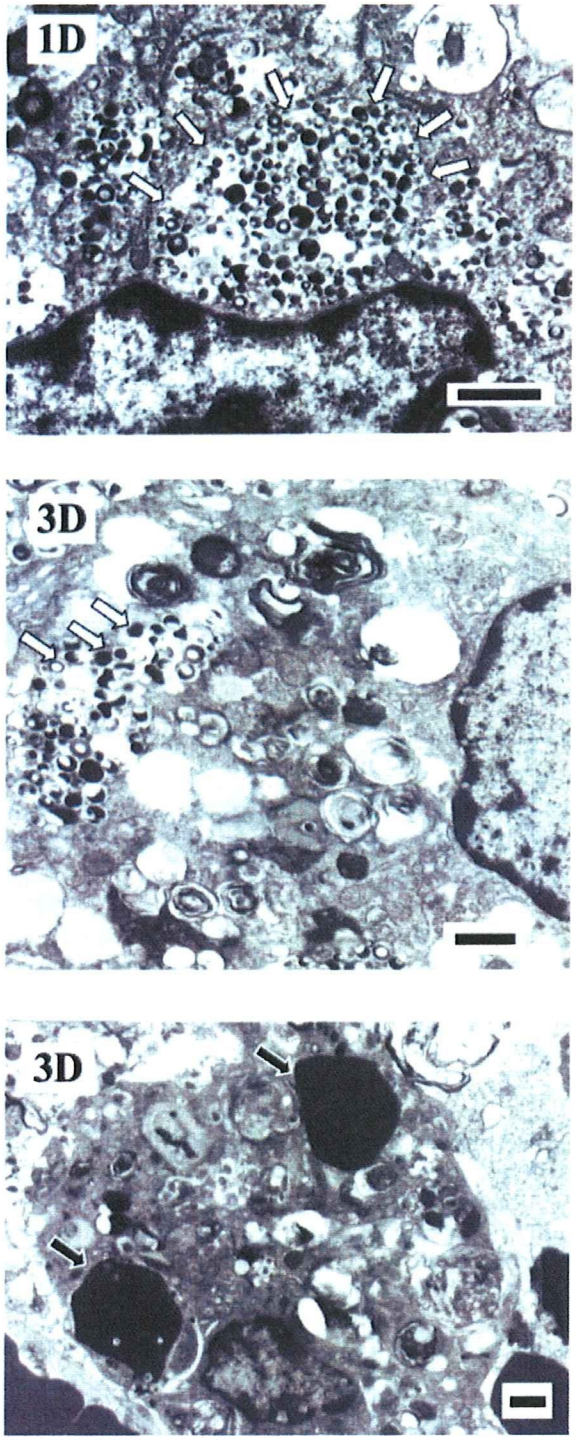

Figure 4. Transmittance electron micrographs of rat brain tissue in the HbV group 1 day and 3 days after intracerebral injection of HbV. The individual HbV particles are visible as black particles in the phagosomes of macrophages at 1 and 3 days, as indicated with white arrows. A macrophage phagocytizing not only HbV but also RBC (black arrows) is visible. Scale bar, 1 μm.

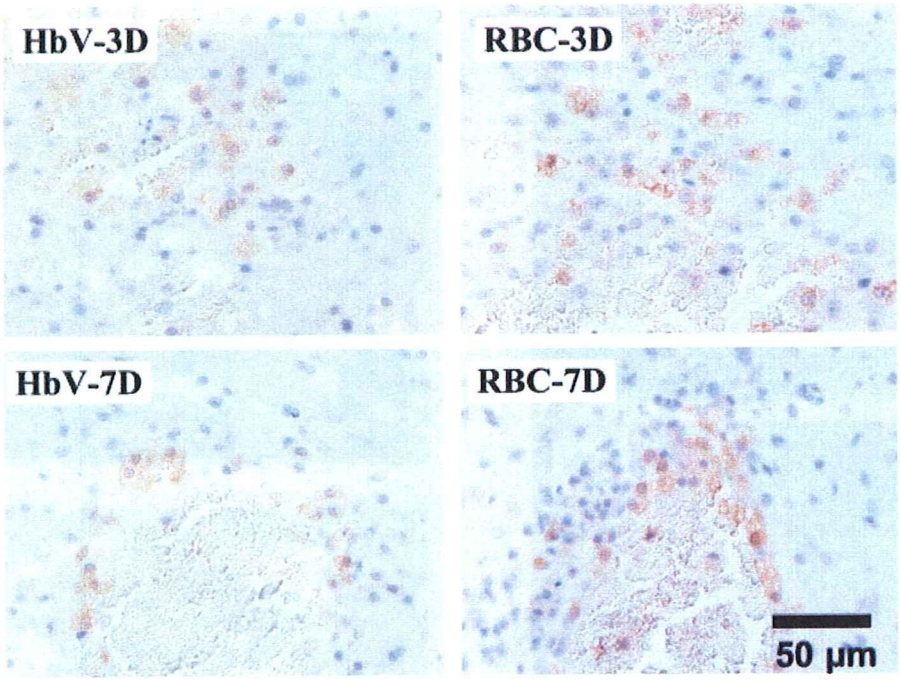

Figure 5. Immunochemical staining with anti-rat HO-1 antibody of rat brain 3 and 7 days after injection of HbV and RBC. Intense staining was confirmed especially at the rim of the perihematoma region. [Color figure can be viewed in the online issue, which is available at www.interscience.wiley.com.]

brain can be a useful approach for fundamental characterization of HbV pathophysiology in ICH.[29] The vesicular size of HbV, 250 μm, is much larger than plasma proteins. It is noteworthy that, in a previous experiment, HbV did not infiltrate into the brain tissue compartment even when a severe hemorrhagic condition was produced experimentally by blood draining and the BBB was damaged while HbV solution was tested as a resuscitation fluid.[4] The current study further investigated possible HbV toxicity produced on brain tissue when it was injected directly into the brain compartment.

Many reports have described the cellular, biochemical, and pathophysiological effects of ICH. In addition, the time course of the effects has been investigated using many animal model systems.[30–34] The intensity and the time course of these debilitating effects of experimentally induced ICH generally paralleled with the intracerebral injection volume.[16,35,36] In our experiment, the volume of injection into a rat brain was small: 20 μL. Precedent studies reported that 20 μL of RBC injection caused brain edema and BBB breakdown at 3 days,[37] and that the mortality rate increased with 30 μL injection.[38] We have anticipated, therefore, that HbV might cause some intense reactions as they were demonstrated with RBC.[35] Additionally, there has been a report demonstrating a close relationship between brain edema and forelimb placing deficit scores after the experimental ICH.[35] For both HbV and RBC groups, the 20 μL injection produced slight signs of motor dysfunctions, that is "miss-steps," "dragging" of the left foot, and the reduction of the forelimb "hanging-time," that is classical striatal motor dysfunctions. The current study used measurements of body weight gain, wet brain weight, and motor dysfunctions. However, all were mutually comparable with the HbV treated animals and with the RBC treated animals; HbV showed no notable adverse reactions over that seen with RBC.

Histopathological examination 1 day after the injection indicated that both HbV and RBC groups showed the infiltration of neutrophils surrounding the hematoma. Neutrophils release various inflammatory cytokines, such as tumor necrosis factor-α, interleukin-6, and interferon-γ, which play important roles in brain damage.[16] The neutrophil infiltration is a normal response to tissue damage such as brain ischemia and traumatic injury.[39] The number of neutrophils had decreased significantly by 3 days in both groups. Immunochemical staining with anti-human Hb antibody showed that a considerable amount of small HbV corpuscles were dispersed into surrounding tissue. In contrast, a large amount of RBC mostly remained in the hematoma. These differences between HbV and RBC might be attributable to the differences in sizes of two corpuscles, or other physicochemical properties for dispersion. It

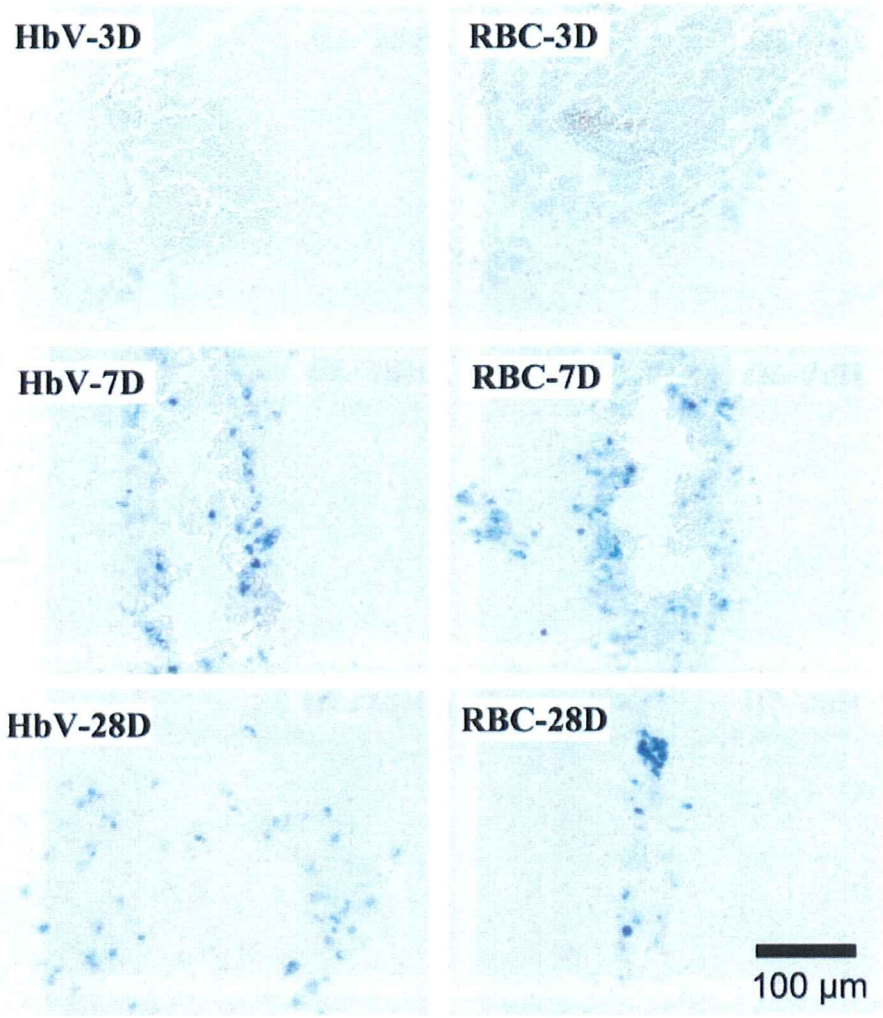

Figure 6. Berlin blue staining of rat brain 3, 7, and 28 days after injection of HbV and RBC. Large amount of hemosiderin deposition was confirmed just near the hematoma site for both groups. Hemosiderin deposition was confirmed at 28 days for both groups. [Color figure can be viewed in the online issue, which is available at www.interscience.wiley.com.]

will be quite important, therefore, to investigate these differences in future studies, in particular, to investigate how the HbV is biodegraded in the brain.

Perihematomal edema might involve in damage to the vascular endothelium. Iron is a potent catalyst of lipid peroxidation; the release of iron (a breakdown product of Hb) after RBC lysis might contribute to BBB damage, brain edema, reduced blood flow, and cell death.[16,18,28,31,40,41] Actually, TUNEL staining demonstrated that both groups had apoptotic cells during the entire period of observation. The strong perihematomal hemosiderin deposition observed in our current study also suggests that they are derived from RBC lysis. However, the fact that the surrounding tissue, infiltrated with HbV, showed no strong hemosiderin deposition compared to that of RBC, could indicate that HbV was more stable and degraded slowly by phagocytosis of the macrophages. This study did not identify whether the macrophages were microglia or those infiltrated from blood through BBB. The phagocytized HbV in the macrophages, however, were clearly present, even at 28 days, by staining with an anti-human Hb antibody.

Degradation of HbV in the brain seemed much slower than those observed in liver Kupffer cells and spleen macrophages after the HbV intravenous injection.[5,13] This gradual degradation might be advantageous clinically to prevent acute toxic effects of Hb molecules. It has been known that phospholipid vesicles (liposomes) are unstable capsules. However, the stability of liposomes depends on the physicochemical characteristics of lipids. Our HbV, com-

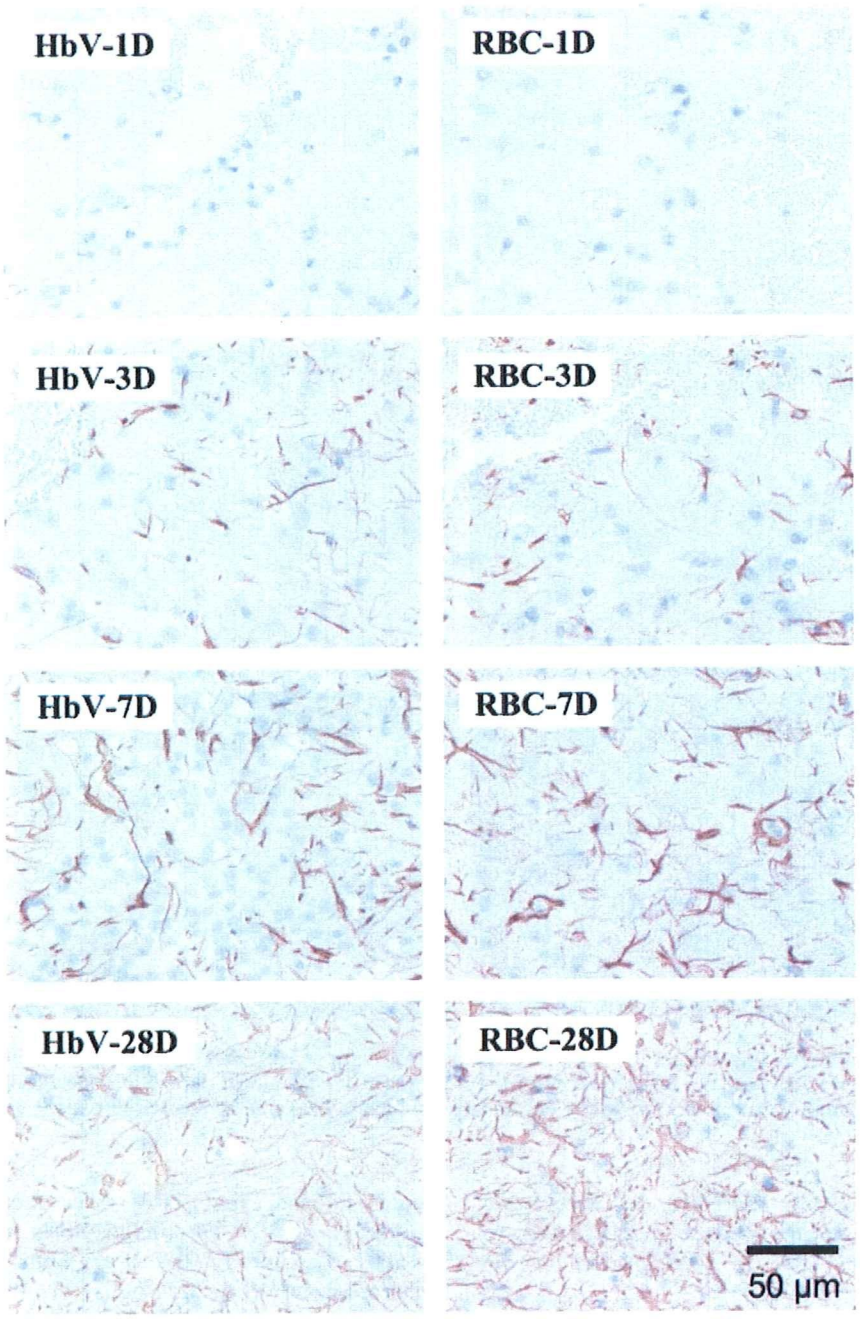

Figure 7. Immunochemical staining with anti-GFAP-staining 1, 3, 7, and 28 days after intracerebral injection of HbV and RBC. On day 1, the initial destruction of astrocytes in the perifocal zone for both groups, and from 3 days a dense network of hypertrophic processes reentered the perifocal zone. At 7 days, the hypertrophic and hyperplastic astrocytes were distributed in a large area. At 28 days, the presence of gliosis was evident in both groups. [Color figure can be viewed in the online issue, which is available at www.interscience.wiley.com.]

posed mainly of DPPC, cholesterol, and PEG-conjugated lipid, has been tested to be enormously stable, as presented in Table II, against physical stimuli by hypotonic shock and freeze-thawing. The process of phagocytosis involves the secretion of PLA_2.[42] The *in vitro* demonstration of HbV resistance to PLA_2 enzymatic lipolysis might support the notion that the HbV is also more resistant to PLA_2 in the brain and shows a lower rate of degradation than RBC. Moreover, it has been reported that DPPC, which com-

TABLE II
Structural Stability of HbV in Comparison with RBC (n = 3)

Stimuli	Hemolysis (%)	
	HbV	RBC
Hypotonic lysis	0.4 ± 0.0	94.0 ± 0.7
Freeze-thawing	20.4 ± 1.2	77.6 ± 1.2
PLA_2, 30 min	0.0 ± 0.0	12.8 ± 0.3
PLA_2, 2 h	0.1 ± 0.0	17.7 ± 0.7

Mean ± SE.
PLA_2, phospholipase A_2.

prises saturated acyl chains, is less subject to lipid peroxidation than the unsaturated phospholipids in biomembranes.[43,44]

Acellular intramolecularly crosslinked Hb solution was clinically tested in stroke patients; production of significant adverse events was reported.[45] The same material was also tested for the treatment of severe traumatic hemorrhage. The mortality rate seemed increased, especially in patients with head injury.[19,26] Even though the mechanism for this adverse response has not been clarified, it is anticipated that Hb molecules (6 nm) smaller than HbV (250 nm) easily infiltrate into the perifocal tissues when the BBB breaks down. The extravasated Hb would directly interact with the cells and potentiate brain damage.[46,47]

Significant morphological changes of astrocytes were observed in our study. Astrocytes are the most numerous cells in the central nervous system. They provide structural, trophic, and metabolic support to neurons and modulate synaptic activities. Impairment in the astrocyte functions during brain ischemia and other insults can critically influence neuron survival.[48] After traumatic injury, surviving astrocytes are well known to begin to exhibit hypertrophy and proliferation.[49,50] In our study, GFAP-immunoreactivity showed that, from 3 days, a dense network of hypertrophic processes appeared in the perifocal zone. At 7 days, the hypertrophic and hyperplastic astrocytes distribute in a large area, replacing the hematoma. At 28 days, the hematoma scar remained as gliosis. This process closely resembles the observations of the RBC group in the current study, and in the reported pathological profile after ICH.[51]

Aside from blood substitute research, phospholipid vesicles or liposomes encapsulating or embedding functional drugs or biological materials have been investigated aggressively for use in drug delivery systems or controlled release; some were subsequently approved for antifungal or anticancer therapy.[52] The BBB presents an obstacle for efficient drug administration using nanocarriers to brain tissue.[53] In fact, intracerebral injection of antitumor drugs encapsulated in liposomes is documented.[54,55] From the viewpoint of biomaterial science, results of the present study assure the safety of the present lipid formulation used for the HbV, and show it to be applicable for drug release systems for intracerebral injection.

In conclusion, intracerebral injection of HbV caused infiltration of HbV into the perihematomal brain tissue and the inflammatory reaction that consist of neutrophil accumulation at the site of injury, subsequent gradual degradation of HbV in macrophages, and hypertrophy of astrocytes to reconstruct the injured tissue. These are all expected to be normal reactions to the injury. Actually, there was no aberrant reaction in comparison to the injection of RBC. On the other hand, the delayed degradation of HbV might benefit tissue reconstruction after treatment with HbV infusion as a resuscitative fluid. Further investigations should follow to show the neurological safety of the lipid components of HbV. Because the HbV remained in the brain at 28 days, further investigations should also include longer period of observation. Our present data provided valuable information related to the safety of HbV and encourage us to proceed to clinical research of HbV as a transfusion alternative.

The authors acknowledge Mr. H. Abe (Dept. of Pathology, Keio University), and Mr. M. Hashizume (Hist Science Laboratory Co., Tokyo) for assistance with immunochemical staining, and Dr. Keitaro Sou (Waseda University) for assistance with animal experiments. This work was supported in part by Health and Labour Sciences Research Grants (Health Science Research Including Drug Innovation), Ministry of Health, Labour and Welfare, Japan. The HbV and rHSA were provided respectively from Oxygenix Co., and Nipro Corp. Of the authors, HS, KK and ET were consultants to Oxygenix Co. Of the authors, HS and ET are holders of patents related to HbV production.

References

1. Kobayashi K, Izumi Y, Yoshizu A, Horinouchi H, Park SI, Sakai H, Takeoka S, Nishide H, Tsuchida E. The oxygen carrying capability of hemoglobin vesicles evaluated in rat exchange transfusion models. Artif Cells Blood Substit Immobil Biotechnol 1997;25:357–366.
2. Yamaguchi M, Fujihara M, Wakamoto S, Sakai H, Takeoka S, Tsuchida E, Azuma H, Ikeda H. Influence of hemoglobin vesicles, cellular-type artificial oxygen carriers, on human umbilical cord blood hematopoietic progenitor cells in vitro. J Biomed Mater Res A 2009;88:34–42.
3. Chang TM. Therapeutic applications of polymeric artificial cells. Nat Rev Drug Discov 2005;4:221–235.
4. Sakai H, Masada Y, Horinouchi H, Yamamoto M, Ikeda E, Takeoka S, Kobayashi K, Tsuchida E. Hemoglobin-vesicles suspended in recombinant human serum albumin for resuscitation from hemorrhagic shock in anesthetized rats. Crit Care Med 2004;32:539–545.

5. Sakai H, Horinouchi H, Yamamoto M, Ikeda E, Takeoka S, Takaori M, Tsuchida E, Kobayashi K. Acute 40 percent exchange-transfusion with hemoglobin-vesicles (HbV) suspended in recombinant human serum albumin solution: Degradation of HbV and erythropoiesis in a rat spleen for 2 weeks. Transfusion 2006;46:339–347.
6. Sakai H, Takeoka S, Yokohama H, Seino Y, Nishide H, Tsuchida E. Purification of concentrated hemoglobin using organic solvent and heat treatment. Protein Expr Purif 1993;4:563–569.
7. Sakai H, Tomiyama KI, Sou K, Takeoka S, Tsuchida E. Poly (ethylene glycol)-conjugation and deoxygenation enable long-term preservation of hemoglobin-vesicles as oxygen carriers in a liquid state. Bioconjug Chem 2000;11:425–432.
8. Naito Y, Fukutomi I, Masada Y, Sakai H, Takeoka S, Tsuchida E, Abe H, Hirayama J, Ikebuchi K, Ikeda H. Virus removal from hemoglobin solution using planova membrane. J Artif Organs 2002;5:141–145.
9. Goda N, Suzuki K, Naito M, Takeoka S, Tsuchida E, Ishimura Y, Tamatani T, Suematsu M. Distribution of heme oxygenase isoforms in rat liver. Topographic basis for carbon monoxide-mediated microvascular relaxation. J Clin Invest 1998;101:604–612.
10. Sakai H, Hara H, Yuasa M, Tsai AG, Takeoka S, Tsuchida E, Intaglietta M. Molecular dimensions of Hb-based O_2 carriers determine constriction of resistance arteries and hypertension. Am J Physiol Heart Circ Physiol 2000;279:H908–H915.
11. Sakai H, Sato A, Masuda K, Takeoka S, Tsuchida E. Hb encapsulation in vesicles retards the reaction with NO, but not CO, by intracellular diffusion barrier. J Biol Chem 2008;283:1508–1517.
12. Sou K, Klipper R, Goins B, Tsuchida E, Phillips WT. Circulation kinetics and organ distribution of Hb-vesicles developed as a red blood cell substitute. J Pharmacol Exp Ther 2005;312: 702–709.
13. Sakai H, Horinouchi H, Tomiyama K, Ikeda E, Takeoka S, Kobayashi K, Tsuchida E. Hemoglobin-vesicles as oxygen carriers: Influence on phagocytic activity and histopathological changes in reticuloendothelial system. Am J Pathol 2001; 159:1079–1088.
14. Sakai H, Masada Y, Horinouchi H, Ikeda E, Sou K, Takeoka S, Suematsu M, Takaori M, Kobayashi K, Tsuchida E. Physiological capacity of the reticuloendothelial system for the degradation of hemoglobin vesicles (artificial oxygen carriers) after massive intravenous doses by daily repeated infusions for 14 days. J Pharmacol Exp Ther 2004;311:874–884.
15. Krizbai IA, Lenzser G, Szatmari E, Farkas AE, Wilhelm I, Fekete Z, Erdos B, Bauer H, Bauer HC, Sandor P, Komjati K. Blood-brain barrier changes during compensated and decompensated hemorrhagic shock. Shock 2005;24:428–433.
16. Xue M, del Bigio MR. Intracerebral injection of autologous whole blood in rats: Time course of inflammation and cell death. Neurosci Lett 2000;283:230–232.
17. Xi G, Hua Y, Bhasin RR, Ennis SR, Keep RF, Hoff JT. Mechanisms of edema formation after intracerebral hemorrhage: Effects of extravasated red blood cells on blood flow and blood-brain barrier integrity. Stroke 2001;32:2932–2938.
18. Huang FP, Xi G, Keep RF, Hua Y, Nemoianu A, Hoff JT. Brain edema after experimental intracerebral hemorrhage: Role of hemoglobin degradation products. J Neurosurg 2002; 96:287–293.
19. Panter SS, Ellington BL, Regan RF. Hemoglobin and neurotoxicity. In: Winslow RM, editor. Blood Substitutes, Chapter 21. London: Elsevier; 2006. p 227–234.
20. Rosenthal G, Morabito D, Cohen M, Roeytenberg A, Derugin N, Panter SS, Knudson MM, Manley G. Use of hemoglobin-based oxygen-carrying solution-201 to improve resuscitation parameters and prevent secondary brain injury in a swine model of traumatic brain injury and hemorrhage: Laboratory investigation. J Neurosurg 2008;108:575–587.
21. Sou K, Naito Y, Endo T, Takeoka S, Tsuchida E. Effective encapsulation of proteins into size-controlled phospholipid vesicles using freeze-thawing and extrusion. Biotechnol Prog 2003;19:1547–1552.
22. Sakai H, Hamada K, Takeoka S, Nishide H, Tsuchida E. Physical properties of hemoglobin vesicles as red cell substitutes. Biotechnol Prog 1996;12:119–125.
23. Sakai H, Hisamoto S, Fukutomi I, Sou K, Takeoka S, Tsuchida E. Detection of lipopolysaccharide in hemoglobin-vesicles by limulus amebocyte lysate test with kinetic-turbidimetric gel clotting analysis and pretreatment of surfactant. J Pharm Sci 2004;93:310–321.
24. Matsubara T, Okuzono H, Senba U. A modification of van Kampen-Zijlstra's reagent for the hemiglobincyanide method. Clin Chim Acta 1979;93:163–164.
25. Hovav E, Halle D, Yedgar S. Viscous macromolecules inhibit erythrocyte hemolysis induced by snake venom phospholipase A_2. Biorheology 1987;23:377–384.
26. Sloan EP, Koenigsberg M, Gens D, Cipolle M, Runge J, Mallory MN, Rodman G Jr. Diaspirin cross-linked hemoglobin (DCLHb) in the treatment of severe traumatic hemorrhagic shock: A randomized controlled efficacy trial. JAMA 1999; 282:1857–1864.
27. Terajima K, Tsueshita T, Sakamoto A, Ogawa R. Fluid resuscitation with hemoglobin vesicles in a rabbit model of acute hemorrhagic shock. Shock 2006;25:184–189.
28. Yoshizu A, Izumi Y, Park S, Sakai H, Takeoka S, Horinouchi H, Ikeda E, Tsuchida E, Kobayashi K. Hemorrhagic shock resuscitation with an artificial oxygen carrier, hemoglobin vesicle, maintains intestinal perfusion, and suppresses the increase in plasma tumor necrosis factor-alpha. ASAIO J 2004;50:458–463.
29. Qureshi AI, Ling GS, Khan J, Suri MF, Miskolczi L, Guterman LR, Hopkins LN. Quantitative analysis of injured, necrotic, and apoptotic cells in a new experimental model of intracerebral hemorrhage. Crit Care Med 2001;29:152–157.
30. Kaufman HH, Pruessner JL, Bernstein DP, Borit A, Ostrow PT, Cahall DL. A rabbit model of intracerebral hematoma. Acta Neuropathol (Berl) 1985;65:318–321.
31. Kobari M, Gotoh F, Tomita M, Tanahashi N, Shinohara T, Terayama Y, Mihara B. Bilateral hemispheric reduction of cerebral blood volume and blood flow immediately after experimental cerebral hemorrhage in cats. Stroke 1988;19:991–996.
32. Wagner KR, Xi G, Hua Y, Kleinholz M, de Courten-Myers GM, Myers RE, Broderick JP, Brott TG. Lobar intracerebral hemorrhage model in pigs: Rapid edema development in perihematomal white matter. Stroke 1996;27:490–497.
33. Gong C, Boulis N, Qian J, Turner DE, Hoff JT, Keep RF. Intracerebral hemorrhage-induced neuronal death. Neurosurgery 2001;48:875–882.
34. Gong Y, Hua Y, Keep RF, Hoff JT, Xi G. Intracerebral hemorrhage: Effects of aging on brain edema and neurological deficits. Stroke 2004;35:2571–2575.
35. Hua Y, Schallert T, Keep RF, Wu J, Hoff JT, Xi G. Behavioral tests after intracerebral hemorrhage in the rat. Stroke 2002;33:2478–2484.
36. Nath FP, Jenkins A, Mendelow AD, Graham DI, Teasdale GM. Early hemodynamic changes in experimental intracerebral hemorrhage. J Neurosurg 1986;65:697–703.
37. Bhasin RR, Xi G, Hua Y, Keep RF, Hoff JT. Experimental intracerebral hemorrhage: Effect of lysed erythrocytes on brain edema and blood-brain barrier permeability. Acta Neurochir Suppl 2002;81:249–251.